nature communications

Article

https://doi.org/10.1038/s41467-024-52372-9

Agnostic B cell selection approach identifies antibodies against *K. pneumoniae* that synergistically drive complement activation

Received: 15 March 2024

Accepted: 2 September 2024

Published online: 16 September 2024

Check for updates

Sjors P. A. van der Lans[1,4], Bart W. Bardoel[1,4], Maartje Ruyken[1], Carla J. C. de Haas[1], Stan Baijens[1], Remy M. Muts[1], Lisette M. Scheepmaker[1], Piet C. Aerts[1], Marije F. L. van 't Wout[1], Johannes Preiner[2], Renoud J. Marijnissen[3], Janine Schuurman[3], Frank J. Beurskens[3], Priscilla F. Kerkman[1] & Suzan H. M. Rooijakkers[1]

Antibody-dependent complement activation plays a key role in the natural human immune response to infections. Currently, the understanding of which antibody-antigen combinations drive a potent complement response on bacteria is limited. Here, we develop an antigen-agnostic approach to stain and single-cell sort human IgG memory B cells recognizing intact bacterial cells, keeping surface antigens in their natural context. With this method we successfully identified 29 antibodies against *K. pneumoniae*, a dominant cause of hospital-acquired infections with increasing antibiotic resistance. Combining genetic tools and functional analyses, we reveal that the capacity of antibodies to activate complement on *K. pneumoniae* critically depends on their antigenic target. Furthermore, we find that antibody combinations can synergistically activate complement on *K. pneumoniae* by strengthening each other's binding in an Fc-independent manner. Understanding the molecular basis of effective complement activation by antibody combinations to mimic a polyclonal response could accelerate the development of antibody-based therapies against problematic infections.

The human complement system plays a key role in the first lines of defense against invading bacteria[1]. It is part of the innate immune system and consists of a family of soluble proteins that form a protective cascade in blood and other body fluids. Although complement activation can be triggered by innate recognition, this process is much more efficient in the presence of specific antibodies. Antibodies can bind to bacteria via their Fragment antigen binding (Fab) arms and interact with the immune system via their Fragment crystallizable (Fc) tail. Antibody-dependent complement activation starts when component C1 binds to antigen-antibody complexes on bacterial surfaces. Optimally, six surface-bound IgG monomers can cluster via Fc-Fc interactions to form a hexamer[2,3]. This hexamer serves as a platform onto which C1 can dock via its six Fc-binding domains, leading to C1 activation and the start of the complement reaction. Complement activation on bacteria results in deposition of the opsonin C3b and the release of the anaphylatoxin C5a, which promote phagocytic uptake and killing by human phagocytes[4]. Furthermore, complement activation induces the formation of lethal membrane attack complex (MAC) pores in the outer membrane of Gram-negative bacteria[5]. Although anti-bacterial antibodies can trigger complement activation, it remains poorly understood why certain antibodies do activate complement but others do not. While antibody binding to the bacterial surface is a prerequisite, it is not known which bacterial surface structures are good targets for an effective complement response. Such basic

[1]Medical Microbiology, University Medical Center Utrecht, Utrecht University, Utrecht, The Netherlands. [2]University of Applied Sciences Upper Austria, Linz, Austria. [3]Genmab, Utrecht, The Netherlands. [4]These authors contributed equally: Sjors P. A. van der Lans, Bart W. Bardoel.
e-mail: s.h.m.rooijakkers@umcutrecht.nl

insights into effective complement activation by anti-bacterial antibodies are important for the development of antibody-based therapies against problematic infections[6,7].

Klebsiella pneumoniae is an important opportunistic human pathogen that frequently causes hospital acquired infections[8]. Of major concern is the strong increase in antibiotic resistance observed among *K. pneumoniae* clinical isolates, making treatment of infections more difficult[9–12]. In 2019 alone, *K. pneumoniae* caused over 700,000 antibiotic resistance associated deaths worldwide, making it the third leading cause of antibiotic resistance associated deaths[13]. As for all Gram-negative bacteria, the outer membrane of *K. pneumoniae* mainly consists of lipopolysaccharide (LPS). LPS is comprised of membrane-anchored lipid A connected to a core oligosaccharide region that is decorated with an O-antigen polysaccharide chain consisting of repeating sugar moieties. The O-antigen can protect *K. pneumoniae* against the complement system by preventing recognition of underlying surface structures, as well as hindering proper MAC formation[14,15]. *K. pneumoniae* can express various O-antigen (O-) types, which differ in molecular composition. Clinically, the O1, O2 and O3 O-types are the most relevant group as they represent 80% of the clinical isolates. In addition, the majority of antibiotic resistant and hypervirulent strains express either the O1 or O2-antigen[16,17]. Another important and highly diverse surface structure of *K. pneumoniae* is the polysaccharide capsule. The capsule plays an important role during infection of *K. pneumoniae*, as it is described to protect against antibody recognition, the complement system and phagocytosis[18–23]. Over 70 different capsule (K-) types have been described to be expressed by *K. pneumoniae*, and many more K-types have been predicted based on genetic diversity of the capsule locus (KL)[16]. An improved understanding of antibody-mediated complement activation on *K. pneumoniae* is crucial for the development of antibody therapies. *K. pneumoniae* primarily infects individuals with an impaired immune system such as neonates, elderly and immunocompromised patients[8,24]. Although their adaptive immune response is compromised, these patients frequently retain a functioning complement system. This implies that development of complement-enhancing antibodies provides an interesting opportunity to boost bacterial clearance by the patient's complement system. However, it remains poorly understood which bacterial antigens should be targeted to mount an effective complement response on *K. pneumoniae*.

Nowadays, memory B cells (mBC's) are the preferred source for antibody discovery as they express membrane-bound antibodies as B cell receptors (BCRs) on their surface[25]. BCR sequencing depends on isolation of antigen-specific B cells using purified antigens as bait for the membrane-bound BCR[26]. Prior efforts to identify human monoclonal antibodies against bacteria have mainly been focused on antibodies that target a single pre-determined antigen. In the case of *K. pneumoniae*, this approach has been successful for identification of high-affinity antibodies against purified O-antigen[17,27]. Selection of B cells with a single antigen prevents that identification of antibodies against other bacterial surface targets. Antibodies directed against different antigens might activate the complement system in a different way. Obtaining antibodies directed to different antigens on the same bacterial strain is required to study differences in antibody-mediated complement activation. This will also help to explore if mixing of different monoclonals, thereby mimicking immune responses during a natural infection, would improve targeting of bacterial cells.

In this paper, we developed an antigen-agnostic approach to identify monoclonal antibodies recognizing the surface of *K. pneumoniae*. Since we do not know which surface antigens trigger potent complement activation, we decided not to pre-select a certain antigen but rather stain B cells with whole bacterial cells, keeping bacterial antigens in their natural context. Using a dual staining method with click-chemistry labeled bacteria, we successfully identified 29 unique antibodies against two clinical *K. pneumoniae* strains. Target-identification and functional studies revealed that the antigenic target on the bacterial surface critically determines the capacity to drive complement activation. Furthermore, analyses of antibody mixtures revealed that some antibodies can act synergistically by enhancing each other's binding to the surface in an Fc-independent manner. Altogether, this work could contribute to a better understanding of antibody-mediated complement activation on bacterial cells, which accelerates the development of effective immune therapies against bacterial infections.

Results

Dual staining of human B cells using intact bacteria identifies 29 antibodies against *K. pneumoniae*

To identify human antibodies that target *K. pneumoniae*, we selected human B cells that recognized fluorescently labeled *K. pneumoniae* via their B cell receptor (BCR). Click chemistry was used to couple fluorescent dyes to lipopolysaccharide (LPS), a conserved cell envelope component of Gram-negative bacteria (Fig. 1a, S1a). This was achieved by growing bacteria in the presence of azide-carrying KDO which incorporates into the LPS and provides a handle for 'clicking' to cyclooctyne-labeled fluorophores. Direct stochastic optical reconstruction microscopy (dSTORM) (Fig. 1a) and flow cytometry (Fig. S1b) demonstrated successful surface labeling of *K. pneumoniae*. Next, we examined whether fluorescently labeled *K. pneumoniae* could be used to identify *K. pneumoniae* specific B cells. We focused on B cells from healthy individuals since previous studies showed they are an effective source for identifying memory B cells against purified *K. pneumoniae* antigens[17,27]. Human B cells were stained by incubation with a mix of two fluorescently labeled bacteria preparations to reduce false positive events in rare event sorting as described for other antigens[28]. B cells that stained positive were detected via flow cytometry. We identified B cells that were single-positive for either ATTO-488 or Cy5 labeled *K. pneumoniae* (Fig. 1b, S1c). In addition, approximately 0.05% of the B cells were double-positive for both ATTO-488 and Cy5 labeled bacteria. Adding an excess of unlabeled *K. pneumoniae* competed primarily with the bacterial staining in the double-positive B cell population, indicating that most single-positive events are cause by background (Fig. S1d, e). Fluorescent microscopy analysis revealed that multiple bacteria were attached to around half of the double-positive sorted B cells (Fig. 1c, S1f). In contrast, the single-positive sorted B cells had almost no bacteria attached. This suggests that the dual staining approach helped to enrich for bacterium-specific B cells. Importantly, the double-positive B cell population was strongly enriched for memory B cells ($CD27^+$), whereas no enrichment was observed within the single-positive populations (Fig. 1b). Together, this suggests that dual staining of B cells with fluorescently labeled intact bacteria allows for the enrichment of *K. pneumoniae*-specific memory B cells.

To prove that the dual staining selects for *K. pneumoniae*-specific B cells, we single-cell sorted double-positive IgG expressing B cells (Fig. 1d; Q2). Next, the VH/VL regions of the sorted B cells were amplified via RT-PCR and cloned into IgG1 expression vectors. Recombinant IgG1 expression in EXPI293F was performed and expression supernatants were collected. To screen for *K. pneumoniae*-specific antibodies, the supernatants were incubated with *K. pneumoniae*, and antibody binding was assessed by flow cytometry (Fig. 1e, S1g). Separate B cell selection rounds were performed with two clinical *K. pneumoniae* isolates (Table S1): *Kpn*O2 (O2a antigen; ST11; KL110) and *Kpn*O1 (O1 antigen; ST219; KL114), which represent the two most dominant O-types among multidrug-resistant *K. pneumoniae*[17]. For *Kpn*O2, a total of 368 double-positive B cells were isolated by single-cell sorting. Screening of expression supernatants revealed 34 positive clones (9.2% success rate) (Fig. 1e). Out of the 34 clones, 12 monoclonal antibodies with a unique CDR3 bound to *Kpn*O2 after large-scale expression and IgG1 purification (Fig. 1f,k, S2a). All 12 clones had undergone somatic hypermutations in both the VH and VL, indicating

https://doi.org/10.1038/s41467-024-52372-9

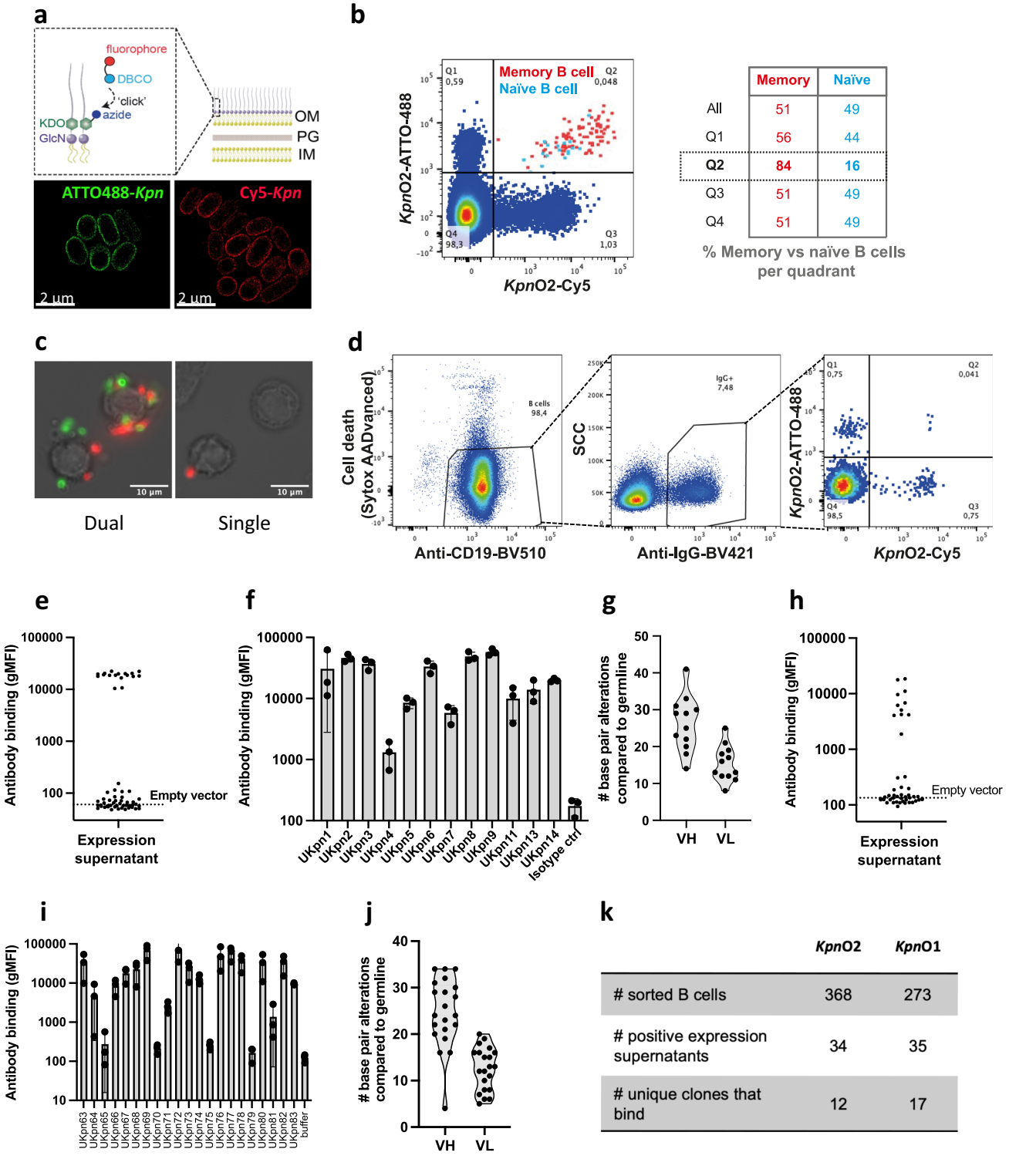

affinity maturation (Fig. 1g, S2a). For *Kpn*O1, a total of 273 double-positive B cells were sorted, yielding 35 expression supernatants that contained antibodies against *Kpn*O1 (12.8% success rate) (Fig. 1h). Out of these, 17 unique monoclonal antibodies bound to *Kpn*O1 as purified IgG1s (Fig. 1i,k, S2b). Finally, we determined that all clones had undergone somatic hypermutation (Fig. 1j). In conclusion, we developed a B cell staining approach to specifically select B cells recognizing entire *K. pneumoniae* bacteria. Using this method, we identified 29 unique human antibodies recognizing two clinically relevant *K. pneumoniae* strains.

Antibodies targeting O2-antigen but not the capsule drive complement activation on *Kpn*O2

Next, we investigated whether the newly identified anti-*K. pneumoniae* antibodies could induce Fc-mediated C3b deposition, a central step in the complement cascade. We first focused on the antibodies recognizing the *Kpn*O2 strain. Purified antibodies were incubated with *Kpn*O2 bacteria and serum of healthy donors (normal human serum (NHS)) as a complement source, and surface deposition of C3b was quantified by flow cytometry. Since NHS contains preexisting antibodies against *K. pneumoniae*, serum was pre-adsorbed with *Kpn*O2 to

Fig. 1 | Dual staining of human B cells with whole bacterial cells identifies 29 IgGs against *K. pneumoniae*. **a** *K. pneumoniae* was cultured overnight in the presence of KDO-azide followed by 'clicking' cyclooctyne-labeled fluorophores to the azide handles. Fluorescent labeling of *Kpn*O2 with Cy5 or ATTO-488 was assessed via dSTORM microscopy. **b**–**d** Dual staining of healthy donor B cells with *Kpn*O2-ATTO-488 and *Kpn*O2-Cy5. **b**, **c** B cells ($CD19^+$) that bound both *Kpn*O2-ATTO-488 and *Kpn*O2-Cy5 were detected by flow cytometry. The double-bacterium-positive (Q2: $ATTO\text{-}488^+$ $Cy5^+$) memory ($CD27^+$) B cells are shown in light blue and the naïve ($CD27^-$) B cells in red. The distribution of memory versus naïve B cells was calculated for the unstained, single stained and dual stained B cells. **c** Double-bacterium-positive B cells were sorted and analyzed for binding of bacteria by fluorescence microscopy. **d** Gating strategy to sort *K. pneumoniae*-specific B cells. Alive B cells ($CD19^+$, death-cell-marker$^-$) that expressed IgG and stained positive for both *Kpn*O2-ATTO-488 and *Kpn*O2-Cy5 were single cell sorted (Q2, right panel). **d**–**i** The heavy and light variable regions (VH and VL, respectively) of single sorted B cells were amplified via RT-PCR and cloned into expression vectors to recombinantly express the antibodies as IgG1 in EXPI293F cells. **e** Antibody binding of 10-fold diluted expression supernatants to *Kpn*O2. **f** The unique *Kpn*O2 antibodies were re-expressed and purified to check binding to *Kpn*O2 (at 1 μg/ml). **g** The VH and VL sequences of unique clones directed against *Kpn*O2 were analyzed for number of base pair alterations compared to germline. **h** Antibody binding of 10-fold diluted expression supernatants to *Kpn*O1. **i** The unique *Kpn*O1 antibodies were re-expressed and purified to check binding to *Kpn*O1 (at 2 μg/ml). **j** The VH and VL sequences of unique clones directed against *Kpn*O1 were analyzed for number of base pair alterations compared to germline. **k** Summary of number of sorted cells, supernatants containing bacterium specific antibodies and unique purified antibody clones. **e**, **f**, **h**, **i** Flow cytometry data are expressed as gMFI values of bacterial populations. **a**–**e**, **h** Data from a single experiment (**f**, **i**) Data represent mean ± SD of three independent experiments.

remove strain specific antibodies (*Kpn*O2ΔNHS) as described previously[29]. Although most identified antibodies against *Kpn*O2 triggered C3b deposition in a dose-dependent manner, for three antibodies (UKpn1, UKpn3, UKpn4, gray lines) we did not observe any C3b deposition, even at the highest tested antibody concentration (Fig. 2a). Four antibodies could very potently induce C3b deposition to levels that were >2-fold over background at 0.1 μg/ml; these 'complement-active' antibodies were colored in dark blue (Fig. 2a,b).

To understand these differences in complement activation, we studied dose-dependent antibody binding to *Kpn*O2 (Fig. 2c). Intriguingly, we observed that the binding of antibodies to the surface of *K. pneumoniae* did not directly correlate with their capacity to activate complement (Fig. 2b,d). For example, we observed that UKpn1 and UKpn3 could potently bind to the *K. pneumoniae* surface (equal to UKpn14) but ineffectively activate complement (Fig. 2b,d). These data indicate that the binding of IgG1 to the surface of *K. pneumoniae* does not automatically lead to Fc-mediated activation of the complement system.

We wondered whether the functional differences between the antibodies could be explained by differences in their target specificity. To identify the bacterial surface targets of the antibodies, we generated a transposon library in *Kpn*O2 using barcoded transposons[30,31] We hypothesized that antibody binding would be lost for mutants in which the transposon disrupts a gene that is involved in surface expression of the antibody target. The transposon library was exposed to either a complement-activating (UKpn2) or a non-activating (UKpn1) antibody, and transposon mutants that were no longer bound by the antibodies were isolated using single-cell sorting of live bacterial cells. We found that approximately 0.5–1% of the transposon mutants were no longer recognized by the antibodies (Fig. S3a). Barcode sequencing of the sorted UKpn1-negative mutants revealed that sixteen unique transposons had inserted in six different genes involved in capsule synthesis (Fig. 2e). Furthermore, sequencing of UKpn2-negative mutants identified twenty unique transposon insertions in five different genes in the *rfb* locus involved in biosynthesis of the O-antigen polysaccharide[26] (Fig. 2f). To confirm these results, we used the lambda-red recombination system to specifically delete the *wbaP* (capsule glycosyltransferase) and *wbbO* (encoding the O-antigen synthesis galactosyltransferase) genes. Indeed, we observed that *Kpn*O2 *ΔwbaP* and *ΔwbbO* deletion mutants were no longer bound by UKpn1 and UKpn2, respectively (Fig. 2g). We analyzed the binding of the other *Kpn*O2-specific antibodies to the *ΔwbaP* and *ΔwbbO* mutants. This revealed that all complement activating antibodies recognized the O-antigen, whereas the antibodies that did not activate complement all target the capsule (Fig. 2g). Additional binding experiments revealed that anti-capsule antibodies recognize another *K. pneumoniae* strain containing the KL110 capsule locus (Fig. S3b). Furthermore, the anti-O-antigen antibodies specifically recognized the O2-antigen, except for antibody UKpn14, which also cross-reacted with an OL104-antigen expressing strain (Fig. S3c). Analysis of antibody binding to bacterial *Kpn*O2 lysate confirmed that UKpn2, 6, 7 and 8 recognize the O-antigen as illustrated by the smear at around 50 kD indicative for the LPS O-antigen (Fig. S3d). In contrast, this staining was absent for UKpn1 and UKpn3 that recognize the capsule.

Various O2-antigen subtypes can be expressed, based on genetic variation within the O locus, as well as the presence of accessory genes. The most common are the O2a and O2afg[16]. O2afg strains have, in addition to the O2a locus, a *gmlABC* gene cluster involved in modifying the O2-antigen[16,32]. While all O2-specific antibodies bound O2a strains, we found that UKpn6 and UKpn7 did not recognize O2afg strains (Fig. S3e). This suggests that the epitopes of UKpn6 and UKpn7 in the O2a antigen are shielded by the O2afg modification. To further specify the difference in the epitopes of UKpn2 and UKpn6, we exposed the *Kpn*O2 transposon library to UKpn2 and UKpn6, and sorted UKpn2-negative mutants that were bound by UKpn6 (Fig. S3f). Transposon sequencing revealed five unique transposon insertions in the gene *orf7*[33] that is located directly downstream of the *rfb* operon (Fig. S3g). This suggests that the galactosyltransferase encoded by *orf7* has a role in O2a biosynthesis that is crucial for binding of UKpn2, but not for UKpn6.

In summary, while the identified antibodies bind to the surface of *K. pneumoniae*, this alone does not result in complement activation. Instead, the specific antigenic target seems to play a crucial role in initiating this process.

Antibodies that target the O1-antigen differ in their potential to drive complement activation

For antibodies targeting the *Kpn*O1 strain, we also assessed the correlation between antibody binding and complement activity. Measuring antibody-dependent C3b deposition revealed that 13 of the 17 antibodies activated the complement system on *Kpn*O1 (Fig. 3a,b). Some antibodies efficiently induce C3b deposition at 0.01 μg/ml, whereas others required a 100-fold higher concentration. Similar to what was observed for *Kpn*O2, we observed that antibody binding (Fig. 3c,d) to *Kpn*O1 did not always correlate with the antibody's capacity to induce C3b deposition. For example, antibodies UKpn80 and UKpn82 showed potent binding to the surface of *Kpn*O1 while hardly inducing complement activation (Fig. 3b,d). Next, we aimed to identify the target of the anti-*Kpn*O1 antibodies. Since the anti-*Kpn*O2 antibodies were all directed against either the O-antigen or the capsule polysaccharide, capsule (Δ*wbaP*) and O-antigen (Δ*wbbO*) deficient mutants of *Kpn*O1 were generated. We observed that all antibodies bound to *Kpn*O1 mutants lacking the *wbaP* capsule gene (Fig. S4). In contrast, antibody binding to the Δ*wbbO* mutant was abrogated, suggesting that all antibodies against *Kpn*O1 targeted the O-antigen (Fig. 3e). Genes involved in the synthesis of the O-antigen are encoded by same locus in O1-antigen and O2-antigen strains[16]. However, O1-antigen strains express two additional genes (*wbbYZ*), which are

https://doi.org/10.1038/s41467-024-52372-9

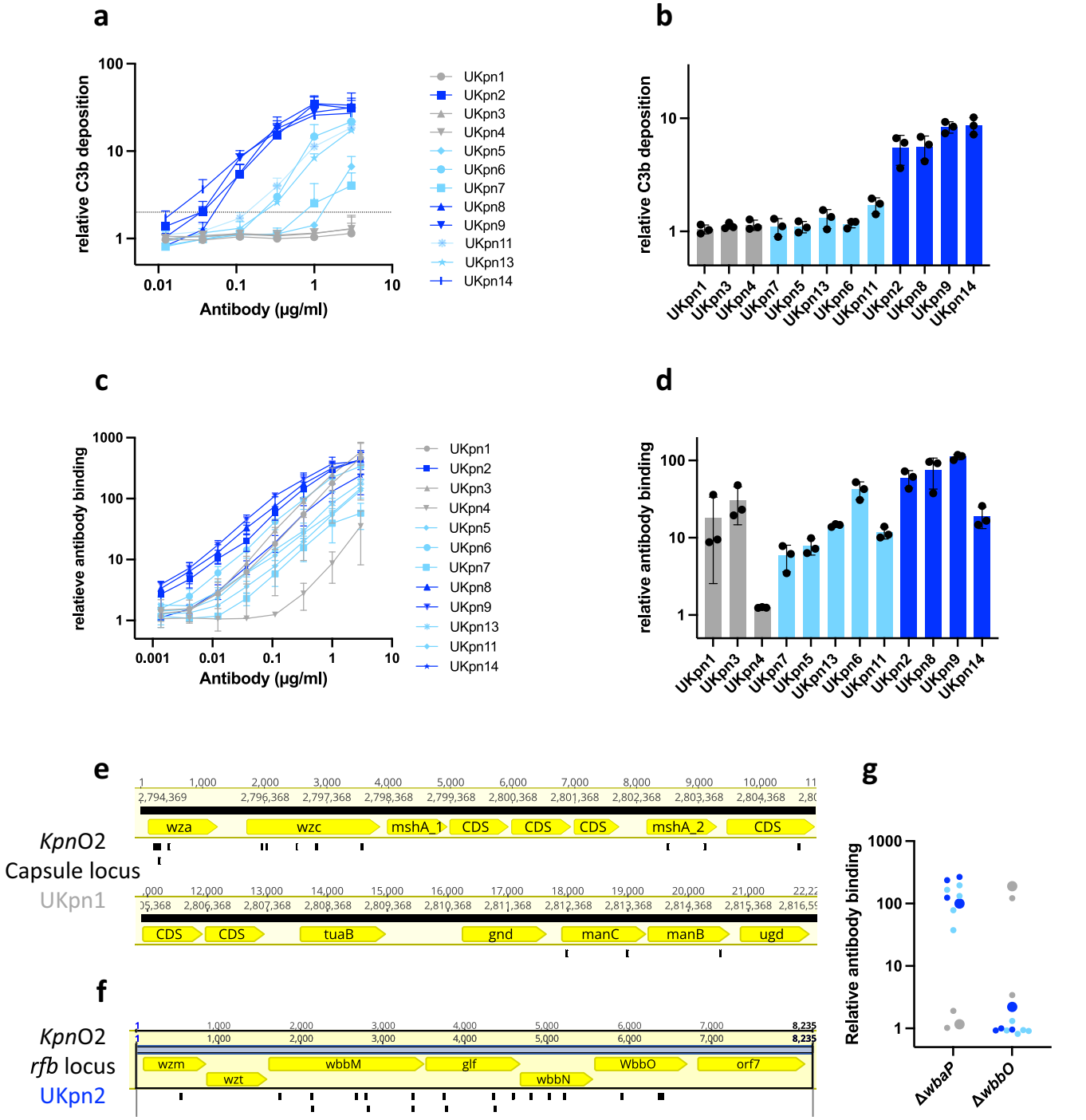

Fig. 2 | Antibodies targeting the O2-antigen but not the capsule drive complement activation on *Kpn*O2. a Antibody-dependent C3b deposition on *Kpn*O2. Bacteria were pre-incubated with a concentration range of *Kpn*O2 IgG1s, followed by addition of 2% *Kpn*O2ΔNHS (NHS depleted from *Kpn*O2 specific antibodies) as a complement source. C3b-deposition was detected using anti-hu-C3b-AF647 by flow cytometry. Potent complement activating antibodies in dark blue (more than 2-fold increase of C3b signal at 0.1 µg/ml indicated by the dotted line), moderate activating antibodies in light blue antibodies and non-complement activating antibodies in gray. **b** Bars represent C3b deposition from (**a**) in the condition where 0.1 µg/ml IgG1 was added, ranked on C3b deposition level. **c** Antibody binding of the different *Kpn*O2 specific antibodies to *Kpn*O2 was detected by flow cytometry and depicted with same color coding as in (**a**). **d** Bars represent antibody binding data from (**c**) at 0.1 µg/ml IgG1. **e**, **f** *Kpn*O2 transposon mutants that are not recognized by (**e**) UKpn1 or (**f**) UKpn2 were single cell sorted. The barcode of the selected mutants was sequenced to determine the location of the transposon insertions (indicated as black bars). **e** Mutants that were no longer bound by UKpn1 had transposon insertions in genes involved in capsule synthesis. **f** Mutants that were not recognized by UKpn2 transposon had insertions in the *rfb* locus. **g** Antibody binding (at 1 µg/ml) to capsule (Δ*wbaP*) and O-antigen (Δ*wbbO*) deletion mutants was measured by flow cytometry and depicted with the same color coding as used in **(a)**, larger dots indicate UKpn1 (gray) and UKpn2 (dark blue). **a**–**d**, **g** Flow cytometry data are represented as relative gMFI of bacterial populations by dividing values by the isotype control. **a**–**d** Data represent mean ± SD of three independent experiments and (**g**) average of 2-3 independent experiments.

https://doi.org/10.1038/s41467-024-52372-9

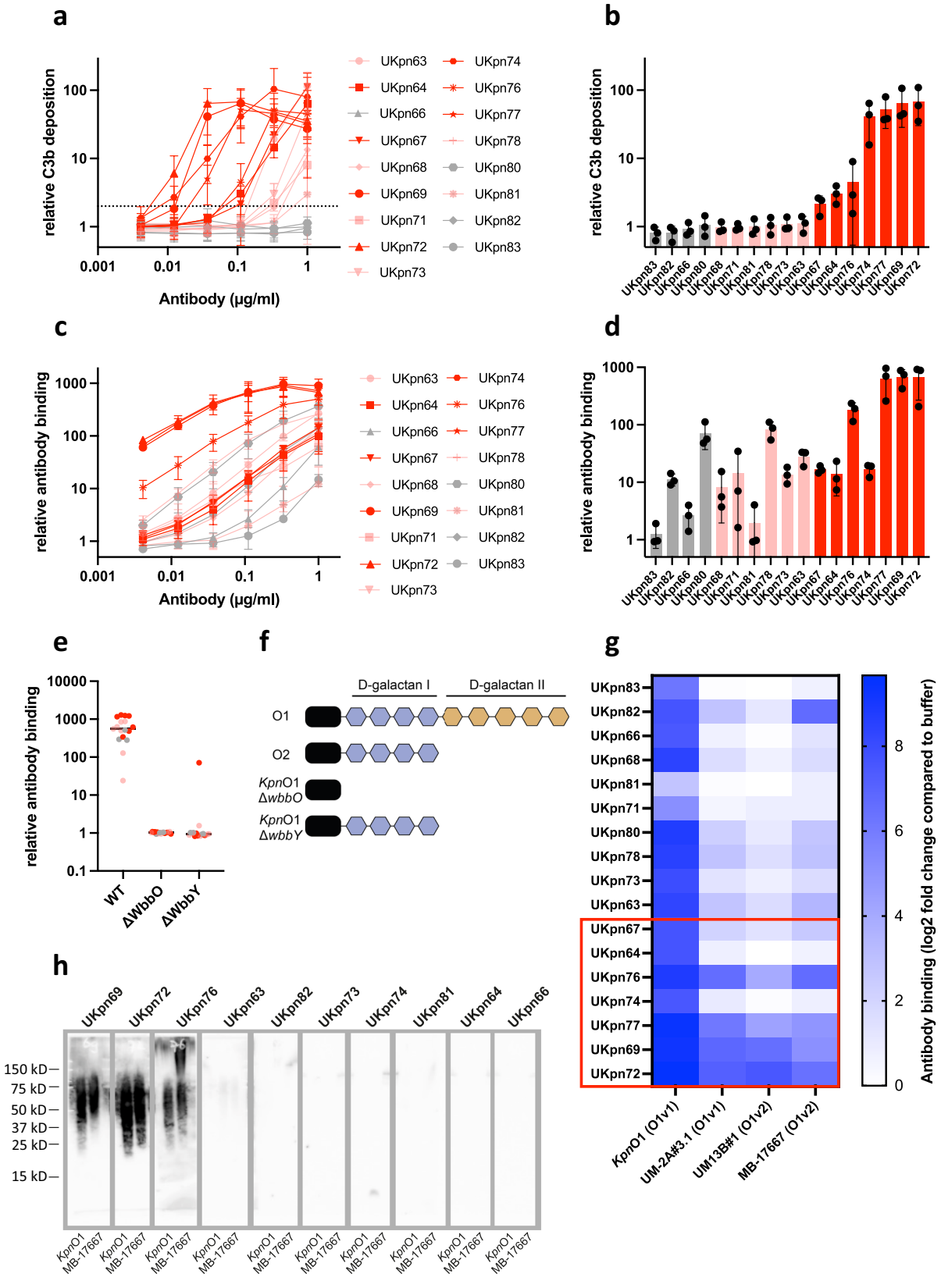

involved in attaching D-galactan-II (O1) on top of a D-galactan-I (O2) segment at the distal part of the O-antigen to form an O1-antigen cap (Fig. 3f)[16]. Upon specific deletion of *wbbY*, we observed that 16 out of 17 antibodies could no longer bind to *Kpn*O1 (Fig. 3e). Strikingly, we found that UKpn69 could still bind to the *Kpn*O1 Δ*wbbY* strain, although with reduced capacity, suggesting that UKpn69 has some affinity for D-galactan-I as well (Fig. 3e). This shows that all the identified anti-*Kpn*O1 antibodies targeted the O1-antigen polysaccharide on *Kpn*O1. We next analyzed whether anti-*Kpn*O1 antibodies could also recognize other O1 strains besides *Kpn*O1. Although most antibodies

Fig. 3 | Antibodies against *Kpn*O1 recognize the O1 antigen and differ in their capacity to drive complement activation. a Antibody-dependent C3b deposition on *Kpn*O1. *Kpn*O1 pre-incubated with anti-*Kpn*O1 IgG1 was incubated with 1% *Kpn*O1ΔNHS (NHS depleted from *Kpn*O1 specific antibodies) as a complement source. C3b-deposition was detected using anti-hu-C3b-AF647 by flow cytometry. Potent complement activating antibodies in dark red (>2-fold increase in C3b deposition at 0.1 μg/ml, indicated by dotted line), moderate complement activating antibodies in light red and non-activating antibodies in gray. **b** Bars represent C3b deposition from (**a**) at 0.1 μg/ml IgG1, ordered based on C3b deposition intensity. **c** Antibody binding to *Kpn*O1 was detected by flow cytometry and depicted with the same color coding as in (**a**). **d** Bars represent antibody binding from **(c)** at 0.1 μg/ml IgG1. **e** Antibody binding (at 1 μg/ml) to *Kpn*O1 wild-type, O-antigen (Δ*wbbO*) and D-galactan II (Δ*wbbY*) was analyzed by flow cytometry. **f** Schematic representation of the LPS O1- and O2-antigen polysaccharide. The O1-antigen consists of D-galactan-II (orange) on top of D-galactan-I (blue), whereas the O2 antigen contains only D-galactan-I. Deletion of the WbbO and WbbY glycosyltransferase leads to the loss of the complete O-antigen and the loss of the distal D-galactan-II part, respectively[16]. **g** Antibody binding (at 1 μg/ml) to different O1-antigen expressing strains was analyzed using flow cytometry. The potent complement activating antibodies are highlighted by the red box (**h**) *Kpn*O1 and an additional clinical strain expressing the O1-antigen (MB-17667) were lysed, and the proteins in the lysate were digested. Western blot was performed using different *Kpn*O1 antibodies followed by goat anti-hu-IgG-HRP. Bands were visualized using ECL. **a**–**e**, **g** Flow cytometry data are represented by gMFI values of bacterial populations that were divided by the buffer control. **g** Data represent log2 transformed data. Data represent (**a**–**d**) mean ± SD or (**e**, **g**) mean of three independent experiments. **h** A representative experiment of two independent experiments is shown.

showed a preference for *Kpn*O1, four antibodies (UKpn69, UKpn72, UKpn76 and UKpn77) could cross-react with all tested O1 strains (Fig. 3g). Interestingly, these four broadly reactive antibodies all belong to the group of potent complement-activating antibodies. Analysis of antibody binding to bacterial lysates showed that only the broadly reactive antibodies could recognize the O1-antigen outside the context of the bacterial cell membrane (Fig. 3h). This suggests that these broadly reactive antibodies recognize the O1-antigen outside the bacterial context. The other *Kpn*O1 antibodies recognize different epitopes in the O1-antigen that are likely better accessible or modified in *Kpn*O1 compared to other O1 strains. Altogether, these data show that identified O1-antigen specific antibodies differ in their capacity to drive complement activation.

Hexamerization-enhancing mutations strongly improve complement activation by anti-capsule antibodies

To understand differences between our complement-active and -inactive antibodies we studied the role of IgG hexamer formation. We hypothesized that the complement-inactive antibodies have a poor capacity to form Fc-dependent hexamers. To study this, we introduced the E430G mutation in the IgG1-Fc domain that can improve Fc-mediated hexamer formation[2]. For *Kpn*O2, we focused on two complement-activating antibodies targeting the O2-antigen (UKpn2 and UKpn6) and two antibodies targeting the capsule (UKpn1, UKpn3) that did not activate complement. For the antibodies targeting the O2-antigen, we observed that hexamerization-enhancing mutations could not enhance C3b deposition in presence of *Kpn*O2ΔNHS (Fig. 4a). In contrast, the same mutations had a very strong impact on the anti-capsule antibodies. Whereas unmutated anti-capsule antibodies do not activate complement at the tested concentrations (<3 μg/ml), introducing the E430G mutation allowed the antibodies to induce C3b deposition at concentrations of 0.3 μg/ml and higher. (Fig. 4b). For *Kpn*01, we found that hexamerization-enhancing mutations showed a moderate enhancement of UKpn72-mediated C3b deposition in presence of *Kpn*O1ΔNHS (Fig. 4c). For UKpn62 and UKpn82 we observed that the E430G mutation did not improve C3b deposition. Altogether, these data demonstrate poor IgG clustering by anti-capsule antibodies which can be enhanced by hexamerization-enhancing mutations.

Antibody-driven C3b deposition results in effective phagocytosis and killing of *K. pneumoniae* by human neutrophils

Next, we studied whether antibodies driving C3b deposition on *K. pneumoniae* also induce downstream phagocytosis and bacterial killing. Since deposited C3b molecules can bind complement receptors on phagocytic cells, we tested whether the antibodies stimulate phagocytosis of GFP-labeled *K. pneumoniae* by human neutrophils in presence of preadsorbed serum. As expected, anti-O2- and anti-O1-antibodies that stimulated C3b deposition also induced phagocytosis in a dose-dependent manner (Fig. 5a,b). In line with the C3b deposition results, phagocytosis of *Kpn*O2 was only observed for the anti-O2-antigen antibodies UKpn2 and UKpn6, but not for the capsule targeting antibodies, UKpn1 and UKpn3 (Fig. 5a). As expected, introduction of the hexamer-enhancing mutations in UKpn1 and UKpn3 strongly enhanced phagocytosis (Fig. S5a). For *Kpn*O1, we found that only the complement activating antibody UKpn72 induced phagocytic uptake of *Kpn*O1 by human neutrophils (Fig. 5b). To test if anti-*K. pneumoniae* antibodies induced neutrophil-mediated killing, we analyzed the number of surviving bacteria and found that the *Kpn*O2 recognizing antibodies UKpn2 and UKpn6 also reduced the number of viable bacteria in the presence of neutrophils (Fig. 5c). For *Kpn*O1, UKpn72 reduced bacterial viability in the presence of neutrophils (Fig. 5d). Next to phagocytosis, C3b deposition could also lead to downstream formation of MAC pores. However, when *Kpn*O2 and *Kpn*O1 were incubated with antibodies and serum in the absence of neutrophils, we observed no decrease in bacterial viability, except a slight decrease for UKpn72 at 0.01 μg/ml (Fig. S5b, S5c). Potentially, a collaboration between MAC and neutrophils[34] at this antibody concentration contributes to the peculiar dose-response of UKpn72 (Fig. 5d). To summarize, we showed that antibody-dependent complement deposition leads to phagocytosis and killing of *K. pneumoniae*.

Anti-capsular antibodies act synergistically in complement activation

Finally, we were curious whether combining different antibodies targeting the same bacterium would affect complement activation on *K. pneumoniae*. We focused on *Kpn*O2, as we have antibodies targeting two different antigens on the same strain (O2-antigen and the capsule). Combining an anti-O2-antigen antibody with an anti-capsule antibody had no effect on complement activation (Fig. S6a). Similarly, mixing two antibodies recognizing the O2 antigen (UKpn2 and UKpn6) did not affect their capacity to drive C3b deposition (Fig. 6a). To our surprise, combining two anti-capsule antibodies (UKpn1 and UKpn3) had a strong impact on complement activation. Whereas the individual anti-capsule antibodies induced limited C3b deposition, mixing the two antibodies potently boosted complement activation with a more than 30-fold increase in efficiency (Fig. 6b). Similar results were obtained using another *K. pneumoniae* strain that expresses the same capsule type (Fig. S6b). Enhanced C3b deposition by the anti-capsule antibody mixture also led to increased phagocytosis (Fig. 6c) and killing of *Kpn*O2 by human neutrophils (Fig. 6d).

We wondered whether the synergistic complement activation could be a result of Fc-mediated hexamer formation. We hypothesized that anti-capsule antibodies would interact with each other via the IgG Fc-tail and form mixed hexameric complexes (also known as hetero-hexamers)[35]. To test this, we used the SpA-B protein, which binds to IgG-Fc domains and thereby prevents IgG1 antibodies to form hexamers[36]. To first verify the activity of SpA-B in the context of

https://doi.org/10.1038/s41467-024-52372-9

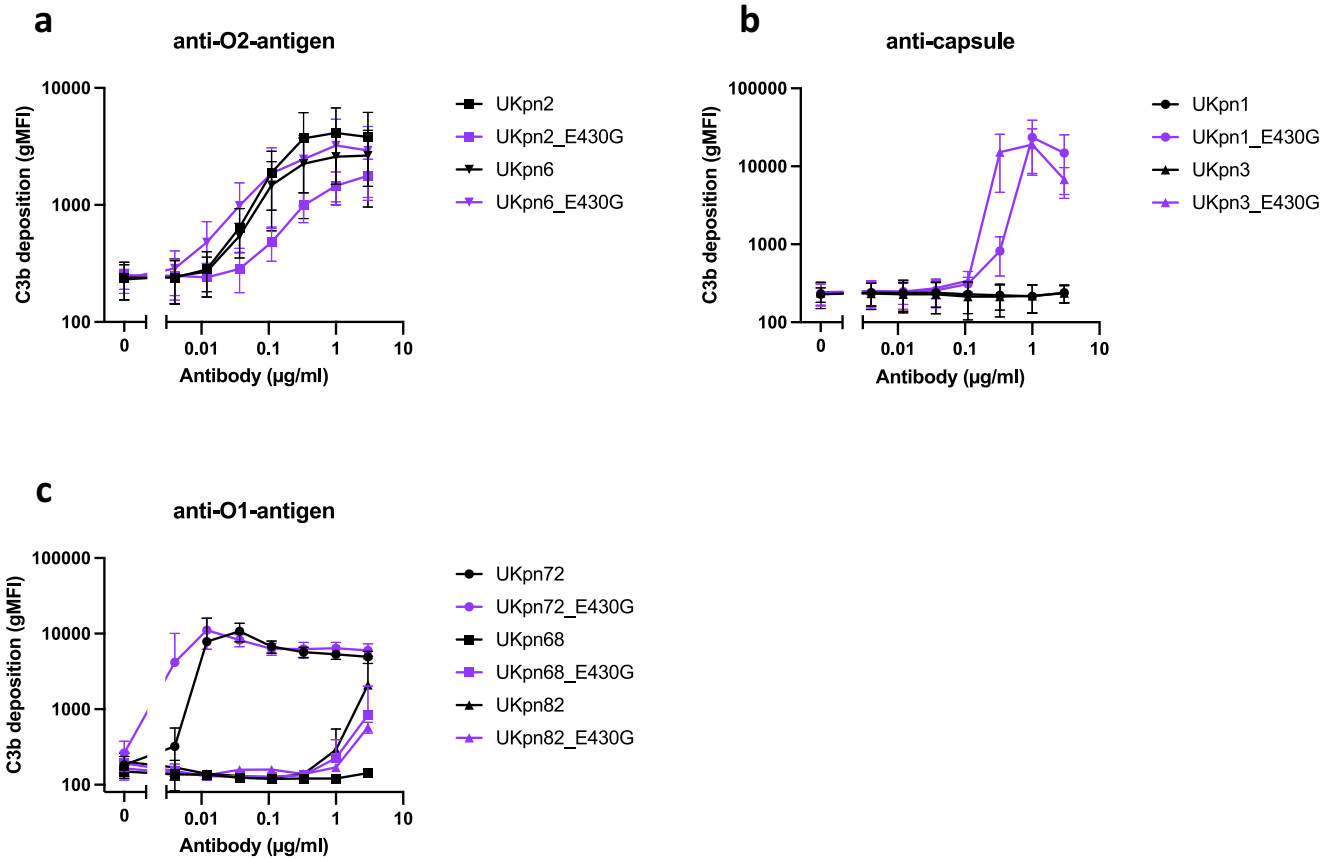

Fig. 4 | Hexamerization-enhancing mutation increases complement activation capacity of anti-capsule antibodies. *Kpn*O2 was incubated with (**a**) anti-O2 antibodies (UKpn2 and UKpn6) as wildtype and E430G variant or (**b**) anti-capsule antibodies (UKpn1 and UKpn3) as wildtype and E430G variant or for 30 min at 4 °C. After antibody binding, bacteria were incubated with 3% *Kpn*O2ΔNHS as a complement source for 30 min at 37 °C. C3b deposition was detected using anti-hu-C3b-A647 and analyzed by flow cytometry. **c** *Kpn*O1 was incubated with the antibodies UKpn72, UKpn68 or UKpn82 as wildtype and E430G variant for 30 min at 4 °C. After antibody binding, bacteria were incubated with 1% *Kpn*O1ΔNHS as a complement source for 30 min at 37 °C. C3b deposition was detected using anti-hu-C3b-A647 and analyzed by flow cytometry. **a**–**c** Flow cytometry data are represented by gMFI of bacterial populations. Data represent mean ± SD of three independent experiments.

*Kpn*O2, we showed that SpA-B fully blocks C3b-depositon induced by an anti-O2 antibody (UKpn2, Fig. 6e). This agrees with previous studies, showing that hexamer formation is important for antibody-dependent complement activation on bacteria[36]. Intriguingly, SpA-B did not effectively reduce C3b deposition induced by the mixture of two anti-capsular antibodies (Fig. 6f), while SpA-B was able to bind to the mixture of UKpn1 and UKpn3 (Fig. S6c). This indicates that the Fc:Fc interactions between neighboring antibodies and ultimately hexamerization does not drive the synergistic activity of these anti-capsule antibodies. In conclusion, we show that mixing two anti-capsule antibodies strongly potentiates their capacity to drive complement activation.

Anti-capsular antibodies strengthen each other's binding in an Fc-independent manner

To gain deeper insight into how anti-capsule antibodies can work synergistically, we analyzed whether the antibodies influence each other's binding to the bacterial surface. For this purpose, anti-capsule antibodies and anti-O2-antigen antibodies were fluorescently labeled and *Kpn*O2 was incubated with a fixed concentration of fluorescent antibody in combination with increasing concentrations of unlabeled antibody. For anti-O2 antibodies, we observed that UKpn2 and UKpn6 compete, indicating they bind a similar epitope, or epitopes that are in proximity of each other (Fig. S7a). Interestingly, mixing the two anti-capsule antibodies did not lead to competition, but showed synergistic binding, as binding of fluorescent UKpn3 was strongly enhanced in the presence of UKpn1 (Fig. 7a). Vice versa, unlabeled UKpn3 also enhanced binding of fluorescent UKpn1 (Fig S7b). Thus, we show that anti-capsule antibodies can jointly activate complement because they strengthen each other's binding to the surface.

We questioned whether the cooperative binding of anti-capsular antibodies was a result of antibodies interacting with each other via the IgG Fc-tails. To this end, we generated divalent F(ab')2 fragments of UKpn1 and UKpn3 by cleavage of full-length IgGs via the IdeS endopeptidase[37] and removal of Fc tails using protein A chromatography (Fig. S7c). Resulting F(ab')2 fragments could still bind to the surface of *Kpn*O2 (Fig. S7d). Next, we tested whether unlabeled F(ab')2 fragments from UKpn1 could strengthen the binding of fluorescent full-length UKpn3 to the surface of *Kpn*O2. Intriguingly, we found that UKpn1-F(ab')2 fragments potently enhanced binding of UKpn3-IgG1 as efficient as UKpn1-IgG on *Kpn*O2 (Fig. 7b). This indicates that the Fc tail is not required to enable cooperative binding with UKpn3. Monovalent Fab fragments of UKpn1 also enhanced binding of UKpn3, but to a lesser extent than F(ab')2 (Fig. 7b). Vice versa, we found that F(ab')2 fragments of UKpn3 also enhanced the binding of fluorescent UKpn1-IgG (Fig. S7e). Furthermore, also combining F(ab')2 fragments of UKpn3 and UKpn1 led to synergistic binding (Fig. 7c, S7f).

Finally, we tested whether $F(ab')_2$ fragments of one antibody strengthen complement activation by the other antibody. As control, we first showed that combining F(ab')2 fragments of UKpn1 and UKpn3 could not induce complement activation on *Kpn*O2 (Fig. 7d), confirming that the antibody's Fc tail is needed for complement

https://doi.org/10.1038/s41467-024-52372-9

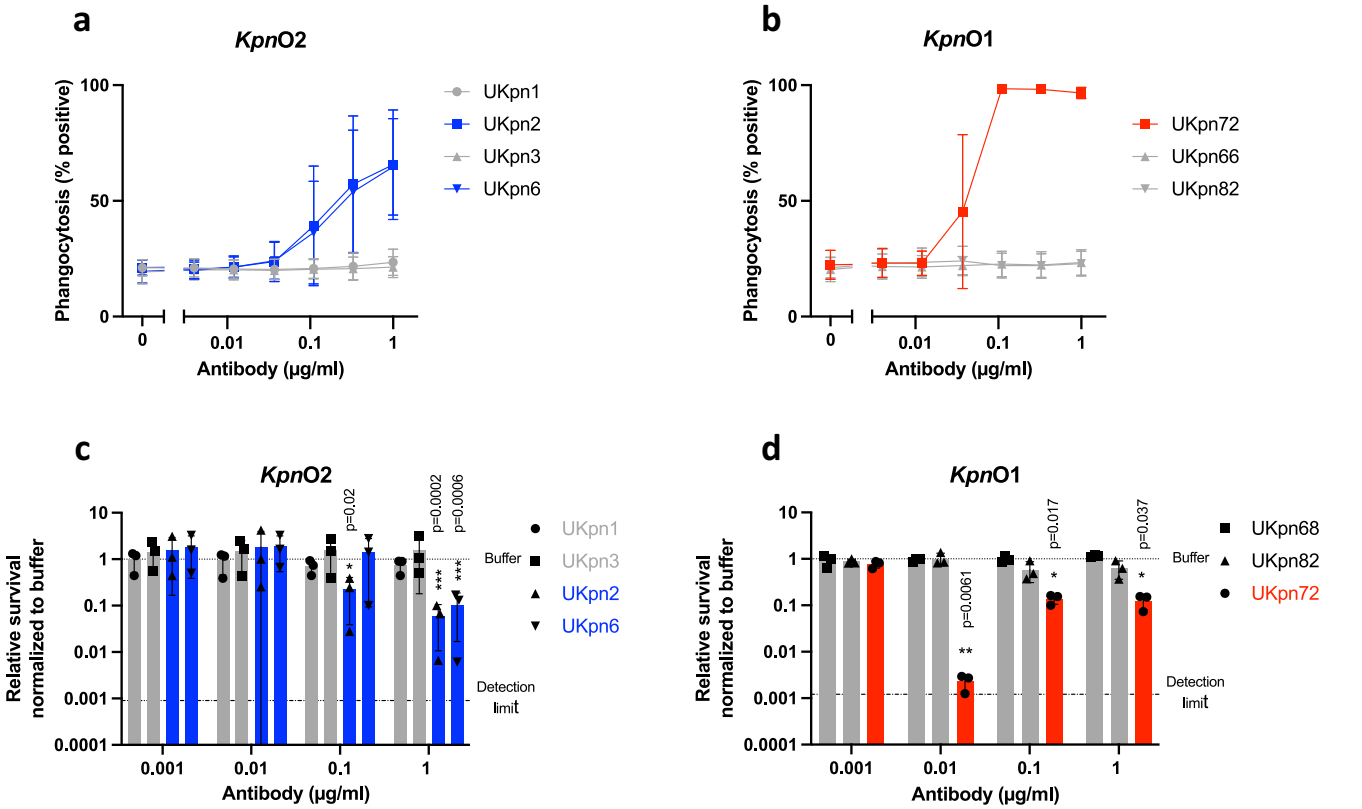

Fig. 5 | Complement activating monoclonal antibodies promote phagocytosis and killing of *K. pneumoniae* by neutrophils. Antibody-dependent phagocytosis of *K. pneumoniae Kpn*O2 (**a**) and *Kpn*O1 (**b**). GFP expressing bacteria were incubated in the presence of antibody and 3% ΔNHS (*Kpn*O2) or 0.5% ΔNHS (*Kpn*O1) as a source of complement. Isolated human neutrophils were allowed to phagocytose opsonized bacteria for 15 min at 37 °C, after which the percentage of GFP-positive neutrophils was determined by flow cytometry. Neutrophil killing of *K. pneumoniae Kpn*O2 (**c**) or *Kpn*O1 (**d**). Bacteria (2×10^5 bacteria/ml) were incubated with antibodies and 8% *Kpn*O2ΔNHS or 1% *Kpn*O1ΔNHS. To this mixture 2×106 neutrophils/ml were added for 3 h at 37 °C. Samples were serially diluted to determine CFU/ml. The data are depicted as relative survival by dividing the CFU/ml values by the no antibody control. **a**–**d** Data represent mean ± SD of three independent experiments. **c**, **d** Data were analyzed by one-way ANOVA with Dunnett multiple comparison analysis compared to without mAb control. Significant differences are indicated, *p < 0.05, **p < 0.01 and ***p < 0.001.

activation. Interestingly, addition of F(ab')2 fragments of UKpn1 strongly enhanced C3b-deposition by full-length UKpn3 and vice versa (Fig. 7d). This strongly suggests that F(ab')2 fragments can also enhance complement activation by a full-length antibody. Altogether, our data demonstrate that the cooperative binding between anti-capsular antibodies occurs via a mechanism that is independent of the Fc-tail.

Discussion

In this study we describe a novel approach to identify human monoclonal antibodies targeting bacterial surface antigens. Using this method, we identified antibodies directed against surface antigens of *K. pneumoniae* and studied the differences in their complement activation potential. Combined, our data suggest that antibody-dependent complement activation is dependent on the surface target and that some, but not all, antibodies can act synergistically.

The main goal of this study was to better understand antibody-dependent complement activation on *K. pneumoniae*. Although antibodies are increasingly considered as an attractive therapy for problematic infections with antibiotic resistant *K. pneumoniae*[7], we still lack basic insights into the molecular determinants that drive potent complement activation. In part, this was due to the lack of a diverse panel of antibodies that recognize the same bacterial strain, and for which the information on the molecular target, binding capacity and complement functionality was known.

Here we identified 29 unique human antibody clones directed against two clinical *K. pneumoniae* strains. For these antibodies, we characterized their complement activity and identified the antigenic target. Although the binding of an antibody to the target surface is the first key step in the complement cascade, we found that binding to *K. pneumoniae* did not automatically trigger complement activation. Clearly, the ability to activate the complement system was influenced by the target antigen. For the O2-antigen strain, we found 12 antibodies targeting the O2-antigen and 3 against the capsule (KL110). Although the binding of antibodies against the O2-antigen and capsule was comparable, we found that all anti-O2-antigen antibodies were able to activate the complement system, whereas the anti-capsule antibodies very weakly activate complement. For the O1 strain, all 17 antibodies recognized the O1-antigen. In contrast to the O2-targeting antibodies, not all anti-O1-antigen antibodies were able to activate complement. Our data suggest that the four most potent antibodies (UKpn69, UKpn72, UKpn76 and UKpn77) recognized a conserved epitope within the O1-antigen. Only these four antibodies were able to cross-react with all four tested O1 strains and could recognize the O1-antigen outside the context of the bacterium.

Our findings that anti-capsular antibodies on the *Kpn*O2 strain weakly activate complement are similar to our previous paper in which we studied antibodies against the capsule of *Streptococcus pneumoniae*[38]. For both *K. pneumoniae* and *S. pneumoniae*, we found that introducing clustering enhancing mutations strongly promoted complement activation by anti-capsule antibodies. Combined, this suggests that anti-capsule antibodies have a poor capacity to form hexameric IgG clusters. It is tempting to speculate that antigenic properties like epitope density determine functional differences

https://doi.org/10.1038/s41467-024-52372-9

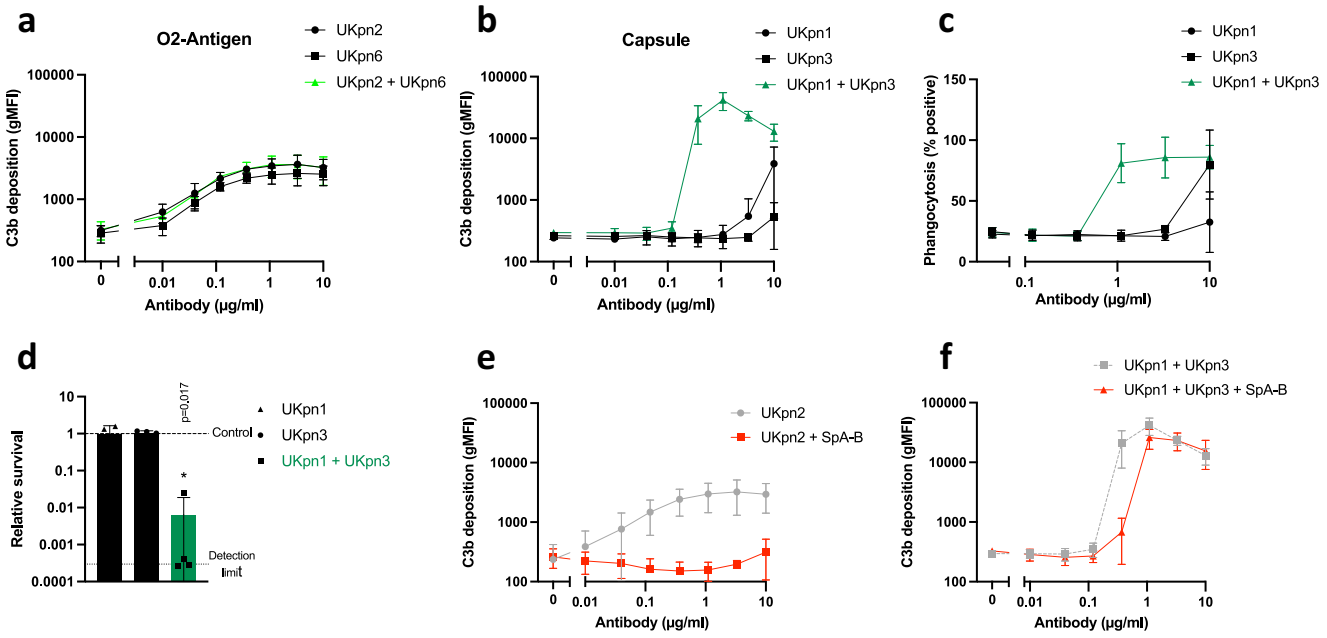

Fig. 6 | Combining capsule targeting antibodies improves complement activation on *Kpn*O2. a, **b** Antibody-dependent C3b deposition. *Kpn*O2 was pre-incubated with antibodies for 30 min at 4 °C. After antibody binding, bacteria were incubated in 3% NHS as a complement source for 30 min at 37 °C. C3b-deposition was detected using anti-hu-C3b-AF647 by flow cytometry. **c** Phagocytosis of *Kpn*O2-GFP by human neutrophils. *Kpn*O2-GFP was incubated with antibodies in the presence of 3% *Kpn*O2ΔNHS. Percentage of neutrophils that phagocytosed was determined by flow cytometry. **d** Antibody-mediated neutrophil killing was analyzed by incubating neutrophils with *Kpn*O2 at MOI of 0.1 together with 8% *Kpn*O2ΔNHS and 0.11 µg/ml antibodies for 2 h at 37 °C. CFU/ml was calculated the next day and expressed as relative survival by dividing with the no antibody control. *Kpn*O2 was pre-incubated with (**e**) UKpn2 or (**f**) the combination of UKpn1 and UKpn3 in the presence or absence of 10 µg/ml SpA-B for 30 min at 4 °C. After antibody binding, 3% NHS as complement source with or without SpA-B was added for 30 min at 37 °C. C3b deposition was measured using anti-hu-C3b-A647 by flow cytometry. **a**–**d**, **f** In the conditions where antibodies were combined, both antibodies were added in the same concentration. The total antibody concentration in the assay is the same for single or combination of antibodies. **a**, **b**, **e**, **f** Flow cytometry data are represented as gMFI values of bacterial populations. **a**–**c**, **e**, **f** Data represent mean ± SD of three independent experiments. **d** Data represents mean ± SD of four independent experiments and were analyzed by one-way ANOVA with Dunnett multiple comparison analysis compared to without mAb control; significant differences are indicated, * $p < 0.05$.

between antibodies targeting capsule versus O2 antigen. Although detailed information for the KL110 capsule is missing, the capsule of *K. pneumoniae* generally consists of a thick (300–500 nm) layer that is covering the bacterial outer membrane (of which the O-antigen is the major component)[39–41]. Also, it has been shown that the capsule is a less dense structure than LPS[39,40]. Therefore, anti-capsular antibodies may be spaced too far apart to efficiently form IgG hexamers via unmutated IgGs. To better understand these differences, further research would be needed to determine the relative surface concentrations, mobility and clustering of capsular polysaccharides versus O2 glycans on *K. pneumoniae*. Alternatively, it could also be that limited accessibility of capsule epitopes prevents efficient oligomerization. Potentially, the capsular polysaccharide is too mobile or structured in such a way that epitopes are hidden.

For all discovered complement-activating antibodies, we observed that C3b deposition on the surface of *K. pneumoniae* induced complement-mediated phagocytosis and killing by human neutrophils. It has previously been shown that anti-O1- and O2-antigen antibodies can induce opsonophagocytosis and are protective in a murine infection model[17]. These studies highlight the importance of complement-dependent phagocytosis in immune defense against *K. pneumoniae*. Since many clinical *K. pneumoniae* strains are MAC resistant[29], opsonophagocytic killing of *K. pneumoniae* using antibodies might be a very important defense mechanism.

Next to understanding monoclonal antibodies, we also aimed to evaluate the functionality of antibody mixtures. In a natural immune response, multiple B cell clones are generated against the invading pathogen. This leads to the production of multiple antibodies that can bind to the same bacterial strain to generate a concerted immune response. Whether anti-bacterial antibodies can act together was yet unknown. Interestingly, we observed that combining two anti-capsule antibody clones led to synergistic binding and complement activation. Initially, we hypothesized that Fc-mediated IgG hexamerization would account for the synergistic binding between anti-capsule antibodies[2,42]. However, the addition of SpA-B, which prevents these interactions[36] could only partially inhibit the synergistic complement activation observed. Furthermore, experiments with F(ab')2 fragments clearly demonstrated that cooperative binding between anti-capsular antibodies is independent of the Fc tails. This strongly suggests that synergistic binding between anti-capsular antibodies is different from previously reported hexamerization mechanisms for IgG1[2,42]. Of note, while synergistic binding between the here described anti-capsule antibodies is independent of Fc, the subsequent complement activation is still mediated by the Fc tail, which forms the docking site for C1q[1].

Although open questions about the exact mechanism behind synergistic binding remain, we currently have two hypotheses. First, we think that antibody binding to one epitope could affect the accessibility of the other epitope. For example, antibody binding to the capsular polysaccharide could induce conformational changes in the local capsule structure that expose otherwise hidden epitopes. Alternatively, the binding of one antibody could stabilize the capsule structure and thereby stimulate binding of antibodies to other epitopes. Second, we speculate that Fab-Fab interactions could play a role. For other anti-glycan antibodies, it has been observed that two Fab domains of one IgG molecule can interact to form intramolecular Fab-Fab dimers[43,44]. Although Fab-Fab interactions between Fab arms of different IgGs has not yet been observed, this could explain

https://doi.org/10.1038/s41467-024-52372-9

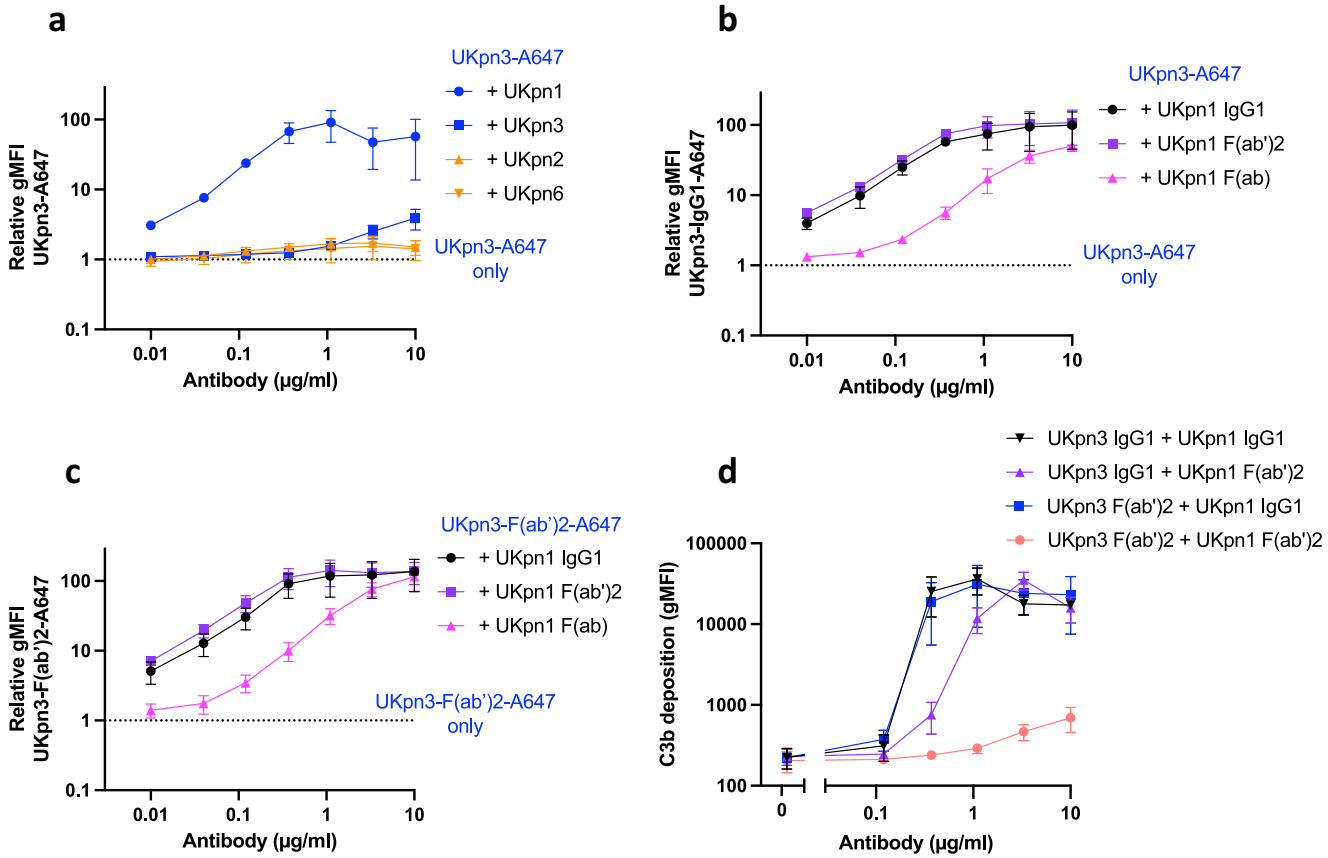

Fig. 7 | Anti-capsular antibodies strengthen each other's binding. *K. pneumoniae Kpn*O2 was incubated with 1 µg/ml directly labeled UKpn3-AF647 (anti-capsule) in the presence of a concentration range of (**a**) IgG1 antibodies (UKpn1, UKpn2, UKpn3 or UKpn6) or (**b**) different variants of UKpn1 (IgG1, F(ab')2 or F(ab)) for 30 min at 4 °C. **c** *K. pneumoniae Kpn*O2 was incubated with 1 µg/ml UKpn3-AF647 F(ab')2 in the presence of a concentration range of different UKpn1 variants (IgG1, F(ab')2 or F(ab)) for 30 min at 4 °C. **a**–**c** Antibody binding was detected by flow cytometry. The relative antibody binding was calculated by dividing the gMFI of the fluorescent antibody in presence of unlabeled antibody variants with the gMFI of the fluorescent antibody only. **d** *K. pneumoniae Kpn*O2 was incubated with combinations of UKpn1 and UKpn3 variants for 30 min at 4 °C, followed by washing and addition of 3% NHS as complement source for 30 min at 37 °C. C3b deposition was measured using anti-hu-C3b-A647 by flow cytometry. **a**–**d** Data represent mean ± SD of three independent experiments.

why the here studied anti-capsular antibodies strengthen each other's binding.

The here described cooperation between antibodies might be an important, but until now overlooked mechanism by which antibodies protect against infections. Interestingly, the two antibody clones mediating synergy were derived from the same donor, indicating they could also act together in vivo. Since our study is limited to in vitro experiments, it remains to be assessed whether the combination of two anti-capsule antibodies is effective in an in vivo infection model. Also, because monoclonal antibodies against other capsular serotypes are still lacking, it remains to be determined whether antibody mixtures targeting other capsular serotypes of *K. pneumoniae* can do the same. Previously, vaccination studies (mainly focusing on K1, K2, K10 and K16 serotypes) have shown that *K. pneumoniae* capsule vaccines elicit an antibody response capable of activating the complement system[45–49]. Since a capsule vaccine induces a polyclonal response[50–52], the combined effects of antibodies in the polyclonal serum could be an important aspect of the protective properties of the described capsule vaccines.

This paper presents a methodology to identify, sequence, and characterize anti-bacterial antibodies using a method to stain human B cells with intact bacteria. The presented method has several advantages compared to the more traditional methods in which bacterial antigens are first isolated and then used to stain B cells. Producing and purifying isolated antigens from bacterial membranes is a laborious and costly process. Importantly, using whole bacteria allows identification of antibodies recognizing antigens in their natural context of the bacterial cell envelope. Indeed, most antibodies identified in this study could recognize the O1-polysaccharide exclusively in the context of whole bacterial cells and not in its isolated form. Vice versa, a previous study using purified antigen as bait for the BCR, identified antibodies that could recognize isolated O-antigens but not whole bacteria expressing that same O-antigen[17]. Finally, as bacteria express a myriad of surface antigens, the use of intact bacteria allows the identification of antibodies against multiple surface antigens. The here presented method has a success rate of around 10 percent, since we retrieved 69 *K. pneumoniae*-specific antibodies (of which 29 were unique) out of 641 sorted B cells. The screening efficacy could be further enhanced when bacterium-specific B cells are cultured after sorting to produce antibody-secreting cells[53,54]. This way, antibodies can be tested functionally before cloning and expression. This would help to prioritize identification of antibodies with strong complement activity and/or recognizing certain targets. The fact that we primarily found antibodies targeting the LPS O-antigen and the capsule indicates that these are the only surface structures accessible for the BCRs. In the future, antibodies recognizing antigens shielded by the O-antigen and capsule[14,21,22] could be identified by performing B cell selections with bacterial strains deficient in O-antigen or capsule[55]. Finally, the source of the B cells could also influence the variety of antibodies. In this study, we focused on B cells from healthy individuals instead of patients. Although the levels of specific memory B cells in circulation are probably lower in healthy individuals, it is easier to obtain large numbers of B cells from healthy donors. Although we find functional

antibodies in healthy individuals, they might have a less diverse repertoire of circulating B cell clones specific for *K. pneumoniae*. Using B cells from patients that recently recovered from a bacterial infection could lead to a wider variety of antibodies. On the other hand, several clinical studies have shown the presence of complement-inhibitory antibodies in patients suffering from severe Gram-negative infections[56,57]. This suggests that the use of patient B cells could also lead to less functional antibodies. The here presented method could help to isolate such non-functional antibodies and further understand their role in bacterial disease.

Because of our antigen-agnostic selection, we included a transposon mutant screening in *K. pneumoniae* to identify the exact genes involved in antibody binding[31]. In this way, we demonstrated that the exact molecular epitopes recognized by the different antibodies varied. Furthermore, this approach also provided insights into the pathway leading to O-antigen synthesis. For example, we found several transposon mutants that no longer bound UKpn2 while retaining UKpn6 binding. These mutants were all affected in the gene *orf7*, indicating that UKpn2 binding critically depends on *orf7* expression. The function of *orf7* is still unknown, but it is predicted to encode for a galactosyltransferase[33], and our data suggests that it may be involved in modifying the O-antigen. Additionally, we observed that UKpn6 and UKpn7 were able to recognize strains expressing the O2a-antigen, but not O2afg-expressing strains. The structure of O2a- and O2afg-antigen is similar, but the O2afg-antigen contains additional 1-4 linked α-D-Galp side groups[58]. This could suggest that UKpn6 and UKpn7 recognize an epitope on O2a that is shielded on O2afg. Furthermore, we observed that UKpn14 bound to the O2-antigen expressing *K. pneumoniae* strains, as well as to a strain that contained the OL104 locus. This was surprising, as the OL104 locus shares sequence similarity with O3- and O5-loci and is therefore predicted to use mannose as the base sugar instead of galactose found in O2-antigens[59].

In conclusion, this work aids in the discovery of antibodies against bacteria and development of therapies to treat *K. pneumoniae* infections. Next to identifying antibodies, our work also shows that combining different antibodies can lead to strong and synergistic enhancement of complement activation on *K. pneumoniae*. This will not only broaden our current understanding of complement activation on bacterial cells but might also be crucial for the development of potent antibody-based therapies to fight bacterial infections.

Methods

Ethics

The work presented in this study complies with all relevant ethical regulations. The use of human blood from healthy volunteers was approved by the Medical Ethics Committee of the University Medical Center Utrecht (METC protocol 07-125/C approved on March 1, 2010). Donors provided informed consent in accordance with the Declaration of Helsinki.

Normal human serum

Normal human serum (NHS) was prepared as described before[5]. Blood was allowed to clot and centrifuged to separate serum from the cellular fraction. Serum of 15–20 donors was pooled and stored at −80 °C. Bacterium depleted NHS (ΔNHS) was prepared as previously described[29] to remove strain specific antibodies without affecting complement activity. Briefly, ice cold NHS was incubated with bacteria to allow bacterium specific antibodies to bind. Bacteria were pelleted and ΔNHS was collected. Three depletion rounds were performed followed by a filtration step. RPMI (ThermoFisher) supplemented with 0.05% human serum albumin (HSA, Sanquin), further referred to as RPMI buffer, was used in all experiments, unless otherwise stated.

Reagents

Phosphate-buffered saline (PBS) was prepared in house, unless otherwise stated. OxEA imaging buffer consisted of PBS supplemented with 50 mM β-mercaptoethylamine hydrochloride (30078, Sigma-Aldrich), 3% (v/v) OxyFluor™ (SAE0059, Sigma-Aldrich) and 20% (v/v) sodium DL-lactate solution (L1375, Sigma-Aldrich), pH 8.0-8.5 (NaOH). MACS buffer consisted of PBS supplemented with 0.5% heat-inactivated fetal calf serum (S181H, Biowest) and 2 mM EDTA (03610, Fluka). B cell culture medium consisted of IMDM (P04-20050, PAN Biotech) and 10% heat-inactivated fetal calf serum (S181H, Biowest). Flow cytometry staining buffer consisted of DPBS (PBS-1A, Capricorn) supplemented with 3% heat-inactivated fetal calf serum (S181H, Biowest). The control antibody aDNP was produced in EXPI293F cells (ThermoFisher)[60].

Bacterial strains

Klebsiella pneumoniae Kp209[61] was kindly provided by Axel Janssen (University Medical Center Utrecht, The Netherlands; University of Lausanne, Switzerland) and will be referred to as *KpnO2*. Clinical *K. pneumoniae* strains, including *KpnO1*, were kindly provided Jelle Scharringa, Jannetta Top and Ad Fluit (University Medical Center Utrecht, The Netherlands). An overview of strains used in this study is included in Table S1. The O-antigen and capsule types (O-type and K-type, respectively) of the *K. pneumoniae* strains were determined based on previously published genome sequences using Kaptive v0.7.3.

Bacterial growth

Unless stated otherwise, *K. pneumoniae* was cultured on Lysogeny broth (LB) 1.5% agar plates at 37 °C. Single colonies were picked and cultured overnight in LB medium at 37 °C while shaking. The following day the bacteria were subcultured by diluting the overnight culture 1:100 in fresh medium and grown to OD_{600} = 0.4–0.5 at 37 °C while shaking. Bacteria were washed twice with RPMI buffer by centrifugation at 10,000 g for 2 min and resuspended to OD_{600} = 0.5 in RPMI buffer.

Fluorescent labeling of bacteria via click-chemistry

Fluorescent labeling of *K. pneumoniae* was based on the labeling method for *E. coli* as previously described[34]. A 1:100 subculture containing 2 μM KDO-N_3 (kindly provided by Pieter de Saint Aulaire and Tom Wennekes, Utrecht University, The Netherlands) was cultured shaking for 16 h at 37 °C. Bacteria were washed twice with ice cold DPBS + 3% FCS, γ-irradiated (10 kGy, Synergy Health, Ede, the Netherlands) and stored at 4 °C. The γ-irradiated bacteria were incubated with 50 μM DBCO-PEG_4-ATTO-488 (CLK-052-05, Jena Bioscience) or DBCO-Cy5 (777374, Sigma-Aldrich) or DBCO-Cy3 (777336, Sigma-Aldrich) for 24 h shaking at 4 °C. Bacteria where then washed twice with DPBS + 3% FCS and labeling was assessed by flow cytometry (MACSQuant, Miltenyi Biotech; or FACSVerse, BD Bioscience).

Generation of *K. pneumoniae*-GFP, *K. pneumoniae*-lux, and *K. pneumoniae* deletion mutants

K. pneumoniae was subcultured to OD_{600} = 0.6-0.8 in 50 ml LB medium, washed twice with 50 ml ice cold milliQ water, and washed twice with 25 ml ice cold 10% glycerol. Bacteria were resuspended in 1 ml 15% glycerol and stored at −80 °C. 50 μl electrocompetent *K. pneumoniae* was mixed with plasmid or PCR product and transformed using a Gene Pulser Xcell electroporation system (Bio-Rad) in a 0.2 cm cuvette (voltage at 2500 V, capacitance at 25 μF, and resistance at 200 Ω). Electroporated bacteria were cultured in 500 μl S.O.C. medium (15544034, Invitrogen) for 60 min at 37 °C, plated on LB agar plates containing the appropriate antibiotics and cultured overnight at 37 °C.

Knockouts were generated using the lambda red method[62]. In brief, primers were designed with 50–60 bp flanking regions up and

downstream of the target gene. The flanking sequences were fused to primers for amplification of a gentamicin resistance cassette. Purified PCR products were electroporated into electrocompetent *K. pneumoniae* cells containing the pREDKI vector[63]. Gentamicin resistant colonies were analyzed for successful deletion of the gene by PCR. To generate *K. pneumoniae* expressing GFP or the lux operon pULTRA-GFP[64] or pUC18-mini-Tn7T-Gm-lux[65] was used for electroporation, respectively. Transformed strains were selected for using 30 μg/ml kanamycin or gentamicin for pULTRA-GFP and pUC18-mini-Tn7T-Gm-lux, respectively.

Widefield microscopy

μ-Slide glass bottom coverslips (80827, Ibidi) were coated with poly-L-lysine solution (P4707, Sigma-Aldrich). B cells that stained positive for *Kpn*O2-Cy5 or double positive for *Kpn*O2-Cy5 and *Kpn*O2-A488 were sorted on top of these coverslips into a 5 μl droplet of DPBS + 2% FCS + 1% paraformaldehyde containing 1.5 μg/ml Dynabeads His-Tag Isolation and Pulldown (10103D, Invitrogen) as a focus point. Cells were analyzed for ATTO488 and Cy5 staining using a Leica SP5 microscope with a HC PL APO 100x/1.40 OIL PH3 objective and GFP (470/40 excitation, 525/50 emission) and Y5 (620/60 excitation, 700/75 emission) filter cubes.

Direct stochastic optical reconstruction microscopy (dSTORM)

μ-Slide glass bottom coverslips were coated with poly-L-lysine solution. Bacteria that were fluorescently labeled via click-chemistry were washed three times in PBS, fixed in 2% PFA (04018-1, Polysciences) + 0.2% glutaraldehyde (G5882, Sigma-Aldrich) and incubated overnight on the coverslip. Immediately before imaging, coverslips were washed three times in PBS and samples were immersed in OxEA imaging buffer. dSTORM imaging was performed using a Nanoimager S Mark II (ONI) at 32 °C at an angle of 52°, using a 488 nm and 640 nm laser at 50% laser power. 10.000 frames were acquired per sample with an exposure time of 30 ms. Images were corrected for drift and filtered using the CODI cloud analysis platform (www.alto.codi.bio, ONI).

B cell isolation

Peripheral blood mononuclear cells (PBMCs) were isolated from buffy coats (E2824R00, Sanquin) using Ficoll-Paque Plus (GE17-1440-02, Cytiva) density gradients (390 g; 20 min). PBMCs were washed by centrifugation (296 g, 10 min) using MACS buffer. Human B cells were isolated from PBMCs using the untouched B cell Isolation Kit II, human (130-091-151, Miltenyi Biotec) by manual separation according to manufacturer's instructions using Pre-Separation Filters (30 μm, 130-041-407, Miltenyi Biotec). Isolated B cells were cryopreserved in B cell culture medium supplemented with 10% dimethylsulfoxide (DMSO, 1.02952, Sigma-Aldrich) and 40% heat-inactivated fetal calf serum (S181H, biowest) at −80 °C in a Mr. Frostry freezing container (5100-0001, Thermo Scientific). Cryopreserved B cells were thawed by added them to B cell culture medium pre-heated to 37 °C, and washed twice by centrifugation (296 g, 10 min, 37 °C). Viable B cells were counted using a TC20 Automated Cell Counter (Bio-Rad) with trypan blue (1450013, Bio-Rad), resuspended to 2×10^6 cells/ml and incubated for 2 h at 37 °C and 5% CO_2.

K. pneumoniae specific B cell stain and single cell sorting

Isolated B cells were washed twice by centrifugation (296 g, 10 min) and resuspended in flow cytometry staining buffer containing combinations of detection antibodies and fluorescently labeled bacteria. Analysis of the dual bacterium staining was analyzed on a FACSVerse instrument using mouse anti-hu-CD19-BV510 (302242, BioLegend) at 1:25, mouse anti-hu-CD27-PE-Cy7 (560609, BD) at 1:200, *Kpn*O2-ATTO-488 and *Kpn*O2-Cy5. Single B cell sorting was performed on different instruments. For the sort using the FACSMelody (BD) instrument mouse anti-hu-CD19-BV510 (302242, BioLegend) at 1:25, mouse anti-hu-IgG-BV421 (562581, BD) at 1:50, *Kpn*O2-ATTO-488 & *Kpn*O2-Cy3 were used. For the sort using the MA900 (Sony) instrument mouse anti-hu-CD19-PE-Cy7 (560728, BD) at 1:200, mouse anti-hu-IgG-BV421 (562581, BD) at 1:50, *Kpn*O2-ATTO-488 and *Kpn*O2-Cy5 was used. For the sort using the Influx cell sorter (BD) instrument mouse anti-hu-CD19-BV510 (302242, BioLegend) at 1:25, mouse anti-hu-IgG-PE-Cy7 (561298, BD) at 1:400, *Kpn*O1-ATTO-488 and *Kpn*O1-Cy5 was used. Bacteria of each fluorescent label were added at a living-B-cell-to-bacterium ratio of 2-to-1, unless stated otherwise. B cells were incubated for 30 min, washed twice by centrifugation (296 g, 10 min), and resuspended in flow cytometry staining buffer. At least five minutes before sorting or measuring the samples in the flow cytometer, Sytox AADvance (R73137, Invitrogen) death cell marker was added at 1:40. *K. pneumoniae*-specific B cells were selected based on the following criteria: single cells, Sytox AADvance$^-$, CD19$^+$, IgG$^+$, and double-bacterium-positive. *K. pneumoniae*-specific B cells were sorted into 96-well PCR-plates containing 10 μl lysis buffer (10 mM Tris pH 8 supplemented with 1 U/μl RNAsin plus RNAse Inhibitor (N2613, Promega)) using a FACSMelody (BD), MA900 (Sony) or Influx cell sorter (BD) instrument. PCR-plates were sealed and stored at −80 °C until further use.

Antibody cloning, expression and purification

Lysed single B cells were thawed to amplify VH and VL regions using the OneStep RT-PCR kit (Qiagen)[66]. Procedure was performed according to manufacturer's protocol with a primer mixture to amplify heavy, kappa and lambda variable sequences[67] (Table S2), primer list, each primer at 20 nM). To each well 15 μl master mix was added and RT-PCR was performed by incubation for 30 min at 50 °C, 15 min at 95 °C, followed by 40 cycles of 1 min at 95 °C, 1 min at 55 °C and 1 min at 72 °C. A second PCR was performed for the amplification of the heavy and light chains separately using 1 μl of the RT-PCR and a mixture of primers containing sequence overhangs required for cloning. The PCR was performed by incubation for 30 s at 98 °C, followed by 40 cycles of 10 s at 98 °C, 20 s at 57 °C and 30 s at 72 °C using HF Phusion DNA polymerase (Thermo Scientific).

For cloning the heavy and light chain amplicons into the expression vectors, 0.5 μl 5-fold diluted heavy chain PCR product and 0.5 μl 5-fold diluted light chain PCR product were mixed with 2 μl of HiFi DNA assembly (NEB) mixture and 1 μl of pcDNA containing the constant region sequences of hu-IgG1, hu-Kappa and hu-Lambda (pFUSE-CHIg-hG1, pFUSE2-CHIg-hK, and pFUSE2-CLIg-hL2, respectively (Invivogen) were cloned separately into pcDNA3.4). The mixture was incubated for 1 h at 50 °C followed by transformation to competent *E. coli* Top10 cells. Transformation was equally divided and added to 1.5 ml LB containing either kanamycin or ampicillin for selection of the heavy chain and light chain expression vectors, respectively. After overnight incubation at 37 °C while shaking, the culture was diluted 1:100 in fresh LB medium containing kanamycin or ampicillin and cultured overnight again. Plasmids were isolated using the PureLink™ *Pro* Quick96 Plasmid Purification Kit (K2110, ThermoFisher) and heavy chain and light chain plasmid were transfected into EXPI293F cells (ThermoFisher, #A14527)[60]. After a 5-day culture, supernatant was harvested and tested for *K. pneumoniae*-specific antibodies using flow cytometry. For expression supernatants that contained antibodies binding to *K. pneumoniae*, the corresponding *E. coli* Top10 transformation cultures containing the heavy and light chain expression vectors were plated to select single colonies to obtain clonal plasmids. Plasmids were isolated from single colonies and the VH and VL sequences were analyzed using Sanger sequencing. Clonal plasmids were used for antibody production in EXPI293F cells followed by purification. Antibodies were purified using a HiTrap protein A column using the AktA Pure (GE Healthare) as previously described[60]. After capture antibodies were eluted according to the manufacturer's instructions and dialyzed overnight against PBS at 4 °C. Purity of proteins was analyzed by SDS-

PAGE followed by staining with Instant Blue (Westburg) and the concentration was determined by OD_{280} measurements. Antibodies selected for follow-up studies in Figs. 4–7 were purified by Size Exclusion Chromatography. All antibodies were stored at 4 °C.

F(ab')2 fragments were generated using the protein His-IdeS, which was recombinantly produced in *E. coli* Rosetta gami and isolated using a His trap column (Cytiva). UKpn1 and UKpn3 were treated His-IdeS (8.4 μg/mg of antibody) for 1 h at 37 °C. Digested antibody was loaded on HiTrap protein A column (Cytiva) to collect the flow-through, which was subsequently loaded on a Histrap column to remove His-IdeS. Flow-through of the Histrap column was collected and loaded on an 30kD centrifugal filter (Amicon) to concentrate F(ab')2 fragments and to exchange the buffer to PBS. Fab fragments specific for UKpn1 and UKpn3 were cloned and expressed similar as the full-length monoclonal antibodies, except that the Fab heavy chain ends with $_{211}$VEPKSC$_{216}$. A flexible linker (GGGGS), followed by the sequence LPETGHH HHHH (his tag) were added at the C-terminus.

IgG1 sequence analysis

IgG genes usage was determined using the IgBlast web tool (Release 1.20.0, NCBI,"https://www.ncbi.nlm.nih.gov/igblast/index.cgi") with standard settings. The heavy and light chain sequences were compared to germline sequences with the highest homology, and used to determine the number of somatic hypermutations, from the start of the framework region 1 (FR1) to the end of the FR3. Deletions and insertions were counted as one mutation. Clonally related sequences were identified on bases of the *IGHV* CDR3 sequence. Translated sequence alignments were created using Genious R9 (v9.1.6)

Antibody binding

Bacteria (OD_{600} = 0.01) were incubated with IgG1 antibodies diluted in RPMI buffer for 30 min at 4 °C under shaking conditions and washed twice by centrifugation with RPMI buffer. Bacteria were resuspended in 1 μg/ml goat anti-hu-IgG-AF647 (2040-31, SouthernBiotech), goat anti-hu-IgG-AF488 (2040-30, SouthernBiotech) or goat F(ab')2 anti-hu-kappa-AF647 (2062-31, SouthernBiotech) for 30 min at 4 °C while shaking. Bacteria were washed twice with RPMI buffer and fixated in 1% paraformaldehyde in PBS for five minutes. Binding was assessed by flow cytometry and expressed as geometric fluorescence intensity (gMFI) of bacterial populations.

Complement deposition

Freshly cultured bacteria (OD_{600} = 0.01) were incubated with antibody diluted in RPMI buffer with 10 μg/ml SpA-B (produced inhouse[36]) only when indicated (30 min, 4 °C, 600 rpm), and washed twice by centrifugation (5 min, 4 °C, 2424 g). Bacteria were resuspended and incubated in NHS or ΔNHS diluted in RPMI buffer with 10 μg/ml SpA-B only when indicated (30 min, 600 rpm, 37 °C). After washing twice, bacteria were incubated with mouse anti-C3b-AF647 (bH6, produced inhouse[5]) (30 min, 4 °C, 600 rpm), washed twice again and fixated with 1% PFA. Fluorescence was detected via flow cytometry.

Conjugation of fluorophores to antibodies and SpA-B

To fluorescently label antibodies and SpA-B, Alexa Fluor 488 NHS Ester (A20000, Invitrogen) or Alexa Fluor 647 NHS Ester (A20006, Invitrogen) was used according to the manufacturer's protocols. Unbound label was removed by buffer exchange into PBS using Zebra Spin desalting columns (40 K, Thermo Scientific), and the degree of labeling was measured. Antibodies were stored at 4 °C.

Transposon screening for antibody target identification

The barcoded Tn5 transposon library in *K. pneumoniae Kpn*O2R was previously described[29]. Coupling of the barcoded transposon to the genomic location was performed using Tnseq[30,31]. Not all barcodes could be allocated indicating that deeper sequencing of the transposon library would yield additional hits. The transposon library was stored at −80 °C. To select for loss-of-binding mutants, the library was thawed on ice, 10-fold diluted and cultured to mid-log (OD_{600} = 0.6). Bacteria were washed by centrifugation in RPMI buffer and resuspended to OD_{600} = 0.02 for UKpn1, and OD_{600} = 0.05 for UKpn2 and UKpn6. Bacteria were incubated with 10 μg/ml antibody conjugated with AF488 or AF647 for 30 min at 4 °C. Bacteria were washed twice by centrifugation in RPMI buffer and analyzed using a Sony MA900 cell sorter. Transposon mutant bacteria that stained negative for the tested antibodies were single cell sorted into 96 wells plates containing LB medium with 30 μg/ml kanamycin. Surviving bacterial clones were rechallenged with the antibodies to confirm that the mutant lacks the epitope required for antibody binding. Barcodes of the validated clones were amplified via colony PCR using Barseq primers[30]. The PCR products were purified and sequenced by Sanger sequencing to identify the barcode of the selected mutant. Transposon insertion sites were visualized in Genious R9 (v9.1.6)

Bacterial lysate western blots

Single bacterial colonies were scraped of agar plates, washed by centrifugation in PBS (2 min 19,000 g), resuspended to OD_{600} = 1.0, and heat-inactivated at 56 °C for one hour. 1 ml heat-inactivated bacteria were pelleted and lysed using Laemmli buffer containing 0.7 M β-mercaptoethanol at 95 °C for 10 min. The proteins in the samples were digested using 400 μg/ml proteinase K for 1.5 h at 60 °C. Proteinase K was inactivated at 95 °C for 5 min, and 5 μl sample was ran over a NuPAGE gel (4%-12% BisTris, NP0323BOX, Invitrogen) for 30 min at 300 V. LPS was transferred to a 0.2 μm PVDF membrane (Bio-Rad) using a Transblot Turbo Transfer system (Bio-Rad). Membranes were blocked overnight at 4 °C using 4% Elk (dried skim milk, Campina), washed and incubated with 1 μg/ml antibody in 1% Elk for 1 h at room temperature. After washing goat anti-hu-IgG-HRP (1:10,000, 2040-05, SouthernBiotech) in 1% Elk was added and incubated for 1 h at room temperature. After washing, the membranes were developed with Pierce ECL Western Blotting Substrate (Thermo Scientific) and images in a LAS4000 Imagequant (GE Healthcare).

Phagocytosis and killing of *K. pneumoniae* by human neutrophils

Human neutrophils were isolated by density gradient as previously described[68]. Concentration of freshly cultured GFP or Lux expressing *K. pneumoniae* (OD_{600} = 0.5) was determined via flow cytometry (MACSQuant). For phagocytosis, 7.5×10^5 GFP-expressing bacteria were incubated with antibody and ΔNHS diluted in RPMI buffer with or without 10 μg/ml SpA-B. After incubation for 15 min at 37 °C, while shaking (750 rpm), 7.5×10^4 human neutrophils were added, and incubated for another 15 min at 37 °C while shaking. Fixation of the samples was performed using 1 % PFA and phagocytosis was measured via flow cytometry. To measure viability, 2×10^4 Lux-expressing bacteria and 2 × 105 neutrophils were incubated in the presence antibody and ΔNHS diluted in RPMI buffer for 3 h at 37 °C. Afterwards the samples were incubated with saponin (0.3%), serially diluted and plated on LB agar. Next day, bacterial colonies were counted to determine the CFU/ml in the samples. The relative survival was calculated by dividing by the no antibody control.

Flow cytometry

Flow cytometry data was analyzed in FlowJo V.10. B cells were gated based on forward and side scatter, death cell marker, and CD19 signal. Bacteria and neutrophils were gated based on forward and side scatter.

Data analysis and statistical testing

Unless stated otherwise data collected as three biological replicates and analyzed using GraphPad Prism version 9.4.1 (458) and Microsoft Excel version 16.87. Statistical analyses are further specified in the figure legends.

Reporting summary

Further information on research design is available in the Nature Portfolio Reporting Summary linked to this article.

Data availability

All data supporting the findings are available in this paper and the Supplementary Information. Source data are provided with this paper.

References

1. Hajishengallis, G., Reis, E. S., Mastellos, D. C., Ricklin, D. & Lambris, J. D. Novel mechanisms and functions of complement. *Nat. Immunol.* **18**, 1288–1298 (2017).
2. Diebolder, C. A. et al. Complement is activated by IgG hexamers assembled at the cell surface. *Science* **343**, 1260–1263 (2014).
3. Abendstein, L. et al. Complement is activated by elevated IgG3 hexameric platforms and deposits C4b onto distinct antibody domains. *Nat. Commun.* **14**, 4027 (2023).
4. Metzemaekers, M., Gouwy, M. & Proost, P. Neutrophil chemoattractant receptors in health and disease: double-edged swords. *Cell. Mol. Immunol.* **17**, 433–450 (2020).
5. Heesterbeek, D. A. et al. Bacterial killing by complement requires membrane attack complex formation via surface-bound C5 convertases. *EMBO J* **38**, e99852 (2019).
6. Theuretzbacher, U., Outterson, K., Engel, A. & Karlén, A. The global preclinical antibacterial pipeline. *Nat. Rev. Microbiol.* **18**, 275–285 (2020).
7. Motley, M. P., Banerjee, K. & Fries, B. C. Monoclonal antibody-based therapies for bacterial infections. *Curr. Opin. Infect. Dis.* **32**, 210–216 (2019).
8. Magill, S. S. et al. Multistate point-prevalence survey of health care-associated infections. *N. Engl. J. Med.* **370**, 1198–1208 (2014).
9. European Centre for Disease Prevention and Control. Antimicrobial resistance in the EU/EEA (EARS-Net) - Annual Epidemiological Report 2021. https://atlas.ecdc.europa.eu/ (2022).
10. Lin, Z., Yu, J., Liu, S. & Zhu, M. Prevalence and antibiotic resistance of *Klebsiella pneumoniae* in a tertiary hospital in Hangzhou, China, 2006–2020. *J. Int. Med. Res.* **50**, 030006052210797 (2022).
11. Bush, K. et al. Tackling antibiotic resistance. *Nat. Rev. Microbiol.* **9**, 894–896 (2011).
12. Laxminarayan, R. et al. Antibiotic resistance—the need for global solutions. *Lancet Infect. Dis.* **13**, 1057–1098 (2013).
13. Murray, C. J. et al. Global burden of bacterial antimicrobial resistance in 2019: a systematic analysis. *Lancet* **399**, 629–655 (2022).
14. Merino, S., Camprubi, S., Alberti, S., Benedi, V. J. & Tomas, J. M. Mechanisms of *Klebsiella pneumoniae* resistance to complement-mediated killing. *Infect. Immun.* **60**, 2529–2535 (1992).
15. Albertí, S. et al. C1q binding and activation of the complement classical pathway by *Klebsiella pneumoniae* outer membrane proteins. *Infect. Immun.* **61**, 852–860 (1993).
16. Lam, M. M. C., Wick, R. R., Judd, L. M., Holt, K. E. & Wyres, K. L. Kaptive 2.0: updated capsule and lipopolysaccharide locus typing for the *Klebsiella pneumoniae* species complex. *Microb. Genom.* **8**, 000800 (2022).
17. Pennini, M. E. et al. Immune stealth-driven O2 serotype prevalence and potential for therapeutic antibodies against multidrug resistant *Klebsiella pneumoniae*. *Nat. Commun.* **8**, 1991 (2017).
18. Fang, C.-T., Chuang, Y.-P., Shun, C.-T., Chang, S.-C. & Wang, J.-T. A novel virulence gene in *Klebsiella pneumoniae* strains causing primary liver abscess and septic metastatic complications. *J. Exp. Med.* **199**, 697–705 (2004).
19. Lin, J.-C. et al. High prevalence of phagocytic-resistant capsular serotypes of *Klebsiella pneumoniae* in liver abscess. *Microbes Infect* **6**, 1191–1198 (2004).
20. Álvarez, D., Merino, S., Tomás, J. M., Benedí, V. J. & Albertí, S. Capsular polysaccharide is a major complement resistance factor in lipopolysaccharide o side chain-deficient *Klebsiella pneumoniae* clinical isolates. *Infect. Immun.* **68**, 953–955 (2000).
21. Domenico, P., Tomas, J. M., Merino, S., Rubires, X. & Cunha, B. A. Surface antigen exposure by bismuth dimercaprol suppression of *Klebsiella pneumoniae* capsular polysaccharide. *Infect. Immun.* **67**, 664–669 (1999).
22. Salo, R. J. et al. Salicylate-enhanced exposure of *Klebsiella pneumoniae* subcapsular components. *Infection* **23**, 371–377 (1995).
23. Domenico, P., Salo, R. J., Cross, A. S. & Cunha, B. A. Polysaccharide capsule-mediated resistance to opsonophagocytosis in *Klebsiella pneumoniae*. *Infect. Immun.* **62**, 4495–4499 (1994).
24. Boyd, A. R. & Orihuela, C. J. Dysregulated inflammation as a risk factor for pneumonia in the elderly. *Aging Dis* **2**, 487–500 (2011).
25. Kurosaki, T., Kometani, K. & Ise, W. Memory B cells. *Nat. Rev. Immunol.* **15**, 149–159 (2015).
26. Wardemann, H. & Busse, C. E. Novel approaches to analyze immunoglobulin repertoires. *Trends Immunol* **38**, 471–482 (2017).
27. Rollenske, T. et al. Cross-specificity of protective human antibodies against *Klebsiella pneumoniae* LPS O-antigen. *Nat. Immunol.* **19**, 617–624 (2018).
28. Gilman, M. S. A. et al. Rapid profiling of RSV antibody repertoires from the memory B cells of naturally infected adult donors. *Sci. Immunol.* **1**, eaaj1879 (2016).
29. van der Lans, S. P. A. et al. Colistin resistance mutations in phoQ can sensitize *Klebsiella pneumoniae* to IgM-mediated complement killing. *Sci. Rep.* **13**, 12618 (2023).
30. Shiver, A. L., Culver, R., Deutschbauer, A. M. & Huang, K. C. Rapid ordering of barcoded transposon insertion libraries of anaerobic bacteria. *Nat. Protoc.* **16**, 3049–3071 (2021).
31. Wetmore, K. M. et al. Rapid quantification of mutant fitness in diverse bacteria by sequencing randomly bar-coded transposons. *mBio* **6**, 1–15 (2015).
32. Clarke, B. R. et al. Molecular basis for the structural diversity in serogroup O_2-antigen polysaccharides in *Klebsiella pneumoniae*. *J. Biol. Chem.* **293**, 4666–4679 (2018).
33. Szijártó, V. et al. Both clades of the epidemic KPC-producing *Klebsiella pneumoniae* clone ST258 share a modified galactan O-antigen type. *Int. J. Med. Microbiol.* **306**, 89–98 (2016).
34. Heesterbeek, D. A. C. et al. Outer membrane permeabilization by the membrane attack complex sensitizes Gram-negative bacteria to antimicrobial proteins in serum and phagocytes. *PLoS Pathog* **17**, e1009227 (2021).
35. Oostindie, S. C. et al. CD20 and CD37 antibodies synergize to activate complement by Fc-mediated clustering. *Haematologica* **104**, 1841–1852 (2019).
36. Cruz, A. R. et al. Staphylococcal protein A inhibits complement activation by interfering with IgG hexamer formation. *Proc. Natl Acad. Sci. USA* **118**, e2016772118 (2021).
37. Von Pawel-Rammingen & Bjorck, L. IdeS and SpeB: immunoglobulin-degrading cysteine proteinases of. *Curr. Opin. Microbiol.* **6**, 50–55 (2003).
38. Aguinagalde Salazar, L. et al. Promoting Fc-Fc interactions between anti-capsular antibodies provides strong immune protection against *Streptococcus pneumoniae*. *Elife* **12**, e80669 (2023).
39. Schembri, M. A., Blom, J., Krogfelt, K. A. & Klemm, P. Capsule and fimbria interaction in *Klebsiella pneumoniae*. *Infect. Immun.* **73**, 4626–4633 (2005).

40. Jensen, T. S. et al. Complement mediated *Klebsiella pneumoniae* capsule changes. *Microbes Infect* **22**, 19–30 (2020).
41. Singh, S. et al. LPS O Antigen plays a key role in *Klebsiella pneumoniae* capsule retention. *Microbiol. Spectr.* **10**, e0151721 (2022).
42. Strasser, J. et al. Unraveling the macromolecular pathways of IgG oligomerization and complement activation on antigenic surfaces. *Nano Lett* **19**, 4787–4796 (2019).
43. Williams, W. B. et al. Fab-dimerized glycan-reactive antibodies are a structural category of natural antibodies. *Cell* **184**, 2955–2972.e25 (2021).
44. Calarese, D. A. et al. Antibody domain exchange is an immunological solution to carbohydrate cluster recognition. *Science* **300**, 2065–2071 (2003).
45. Wantuch, P. L. et al. Heptavalent O-antigen bioconjugate vaccine exhibiting differential functional antibody responses against diverse *Klebsiella pneumoniae* isolates. *J. Infect. Dis.* https://doi.org/10.1093/infdis/jiae097 (2024).
46. Lin, T.-L. et al. Development of *Klebsiella pneumoniae* capsule polysaccharide-conjugated vaccine candidates using phage depolymerases. *Front. Immunol.* **13**, 843183 (2022).
47. Malachowa, N. et al. Vaccine protection against multidrug-resistant *Klebsiella pneumoniae* in a nonhuman primate model of severe lower respiratory tract infection. *mBio* **10**, e02994–19 (2019).
48. Ravinder, M. et al. A synthetic carbohydrate-protein conjugate vaccine candidate against *Klebsiella pneumoniae* serotype K2. *J. Org. Chem.* **85**, 15964–15997 (2020).
49. Kobayashi, S. D. et al. Antibody-mediated killing of carbapenem-resistant ST258 *Klebsiella pneumoniae* by human neutrophils. *mBio* **9**, e00297–18 (2018).
50. Postal, J. M., Gysin, J. & Crenn, Y. Protection against fatal *Klebsiella pneumoniae* sepsis in the squirrel monkey *Saimiri sciureus* after immunization with a capsular polysaccharide vaccine. *Ann. Inst. Pasteur Immunol.* **139**, 401–407 (1988).
51. Cryz, S. J., Fürer, E. & Germanier, R. Safety and immunogenicity of *Klebsiella pneumoniae* K1 capsular polysaccharide vaccine in humans. *J. Infect. Dis.* **151**, 665–671 (1985).
52. Edelman, R. et al. Phase 1 trial of a 24-valent Klebsiella capsular polysaccharide vaccine and an eight-valent Pseudomonas O-polysaccharide conjugate vaccine administered simultaneously. *Vaccine* **12**, 1288–1294 (1994).
53. Sokal, A. et al. Analysis of mRNA vaccination-elicited RBD-specific memory B cells reveals strong but incomplete immune escape of the SARS-CoV-2 Omicron variant. *Immunity* **55**, 1096–1104.e4 (2022).
54. Luo, X. M. et al. Engineering human hematopoietic stem/progenitor cells to produce a broadly neutralizing anti-HIV antibody after in vitro maturation to human B lymphocytes. *Blood* **113**, 1422–1431 (2009).
55. Wang, Q. et al. Target-agnostic identification of functional monoclonal antibodies against *Klebsiella pneumoniae* multimeric MrkA fimbrial subunit. *J. Infect. Dis.* **213**, 1800–1808 (2016).
56. Wells, T. J. et al. Increased severity of respiratory infections associated with elevated anti-LPS IgG2 which inhibits serum bactericidal killing. *J. Exp. Med.* **211**, 1893–1904 (2014).
57. Coggon, C. F. et al. A novel method of serum resistance by *Escherichia coli* that causes urosepsis. *mBio* **9**, 00920–18 (2018).
58. Kelly, R. F., Perry, M. B., Maclean, L. L. & Whitfield, C. Structures of the O-antigens of Klebsiella serotypes 02 (2a,2e), 02 (2a,2e,2h), and 02 (2a,2f,2g), members of a family of related D-galactan O-antigens in Klebsiella spp. *J. Endotoxin Res.* https://doi.org/10.1177/096805199500200208 (1995).
59. Follador, R. et al. The diversity of Klebsiella pneumoniae surface polysaccharides. *Microb. Genom.* **2**, e000073 (2016).
60. Zwarthoff, S. A. et al. C1q binding to surface-bound IgG is stabilized by $C1r_2s_2$ proteases. *Proc. Natl Acad. Sci. USA* **118**, e2102787118 (2021).
61. Janssen, A. B. et al. Evolution of colistin resistance in the *Klebsiella pneumoniae* complex follows multiple evolutionary trajectories with variable effects on fitness and virulence characteristics. *Antimicrob. Agents Chemother.* **65**, e01958–20 (2020).
62. Datsenko, K. A. & Wanner, B. L. One-step inactivation of chromosomal genes in *Escherichia coli* K-12 using PCR products. *Proc. Natl Acad. Sci. USA* **97**, 6640–6645 (2000).
63. Yang, J. et al. High-efficiency scarless genetic modification in *Escherichia coli* by using lambda red recombination and I-SceI cleavage. *Appl. Environ. Microbiol.* **80**, 3826–3834 (2014).
64. Mavridou, D. A. I., Gonzalez, D., Clements, A. & Foster, K. R. The pUltra plasmid series: a robust and flexible tool for fluorescent labeling of Enterobacteria. *Plasmid* **87–88**, 65–71 (2016).
65. Damron, F. H. et al. Construction of mobilizable Mini-Tn *7* vectors for bioluminescent detection of Gram-negative bacteria and single-copy promoter *lux* reporter analysis. *Appl. Environ. Microbiol.* **79**, 4149–4153 (2013).
66. Smith, K. et al. Rapid generation of fully human monoclonal antibodies specific to a vaccinating antigen. *Nat. Protoc.* **4**, 372–384 (2009).
67. Tiller, T. et al. Efficient generation of monoclonal antibodies from single human B cells by single cell RT-PCR and expression vector cloning. *J. Immunol. Methods* **329**, 112–124 (2008).
68. Surewaard, B. G. J., van Strijp, J. A. G. & Nijland, R. Studying Interactions of *Staphylococcus aureus* with neutrophils by flow cytometry and time lapse microscopy. *J. Vis. Exp.* https://doi.org/10.3791/50788 (2013).

Acknowledgements

This work was funded by the Netherlands Organization for Scientific Research (NWO) through a TTW-NACTAR Grant #16442 (to SHMR), Genmab BV, and the European Research Council (ERC) under the European Union's Horizon 2020 research and innovation program (grant agreement no. 101001937, ERC-ACCENT, to SHMR). The authors would like to thank Axel Janssen, Jelle Scharringa, Jannetta Top and Ad Fluit for providing the *K. pneumoniae* strains used in this study, and Pieter de Saint Aulaire and Tom Wennekes for providing KDO-azide, and Pim van Hespen for his help with O- and K-type analysis using Kaptive v0.7.3.

Author contributions

F.J.B., J.S., R.J.M., and S.H.M.R. acquired funding and were involved in study design. S.P.A.vdL., P.F.K., S.H.M.R., B.W.B. conceived the project. P.F.K. and S.P.A.vdL. optimized dual bacterium B cell staining and performed flow cytometry analyses. S.P.A.vdL., P.F.K. and R.M.M. performed B cell sorts. M.R., C.J.C.dH., L.M.S., and P.C.A. cloned expressed and generated antibodies. B.W.B, P.F.K., and S.P.A.vdL. performed sequence analysis. S.P.A.vdL., M.R. performed antibody binding experiments and C3b deposition. B.W.B. and S.B. performed the transposon screens and analysis. M.F.L.vtW. performed widefield and dSTORM microscopy. C.J.C.dH. and M.R. generated *K. pneumoniae* deletion mutants. M.R. performed neutrophil assays and western blots. J.P. analyzed data and gave conceptual advice. S.P.A.vdL. B.W.B., and S.H.M.R. wrote the manuscript. All authors read and approved the submitted version.

Competing interests

R.J.M., J.S., and F.J.B. are (former) employees at Genmab BV and have ownership interests (including stocks, warrants, patents, etc.). Other authors declare no competing interests.

Additional information

Supplementary information The online version contains supplementary material available at https://doi.org/10.1038/s41467-024-52372-9.

Correspondence and requests for materials should be addressed to Suzan H. M. Rooijakkers.

Peer review information *Nature Communications* thanks Tim Rollenske, David Rosen and Ingmar Schoen for their contribution to the peer review of this work. A peer review file is available.